HMA1 and HMA6 are essential components of metal homeostasis in *Arabidopsis thaliana*

by

Ana María Avalos

A Thesis

Submitted to the Faculty of the

WORCESTER POLYTECHNIC INSTITUTE

in partial fulfillment of the requirements for the

Degree of Master of Science

In Biochemistry

April 2004

APPROVED:

Dr. José Argüello, Major Advisor

Dr. James Dittami, Head of Department

TABLE OF CONTENTS

ABSTRACT

Metal homeostasis in plants is regulated by diverse mechanisms that act together to maintain optimal metal ion concentrations inside the cell. P_{1B}-ATPases are heavy metal transport ATPases that are likely to be related to these processes. The sequencing of the genome of *Arabidopsis thaliana* revealed the presence of eight putative P_{1B}-ATPases, HMA1-8.

The main goal in this work is to characterize of the role of P_{1B}-ATPases in plant metal homeostasis. Toward this goal, the P_{1B}-ATPases HMA1 and HMA6 from *Arabidopsis thaliana* were cloned from leaves and sequenced. Results from RT-PCR experiments show ubiquitous expression *in planta* of this two ATPases, except for HMA1 that does not express in roots. Upon Cu^{2+} exposure during growth, expression of HMA6 increases in seedlings. HMA1 expression increases when seedlings are grown in high Cu^{2+} and Co^{2+} media, and decreases when grown in high concentrations of Zn^{2+} and Ni^{2+}. *hma1-1* plants have smaller size and less chlorophyll content than WT plants. Growth is affected in *hma1-1* seedlings when grown in Zn^{2+}, Mn^{2+}, Fe^{2+}, Co^{2+} and Cu^{2+} deficient media, or when these metals are in excess. Moreover, *hma1-1* plants show an increase in Zn^{2+}, Mn^{2+} and Fe^{2+} content in whole plants compared to WT plants. Mutant plants also show increased levels of HMA3 and HMA4 transcripts (Zn^{2+}/Cd^{2+}/Pb^{2+} P_{1B}-ATPases), upregulation of metallothioneins 1a and 2b, downregulation of metallothionein 1c, and a decrease in the phytochellatin synthases 1 and 2 transcripts, compared to WT plants. Homozygous for mutation in HMA6 seems to be lethal, given that none was recovered after screening. These results indicate HMA1 and HMA6 as essential components of plant metal homeostasis in *Arabidopsis thaliana*.

ACKNOWLEDGMENTS

First and foremost, I would like to thank my advisor, Dr. José Argüello for his constant attention and concern so we could receive, as Graduate Students, the best formation. I would also like to thank him for the help received during my first weeks in the US.

Thanks also to Professors Craig Fairchild and Kristin Wobbe, and Prof. Elsbeth Walker from UMass Amherst, for their help and advice during research.

To Dr. James Dittami, Head of Department, for his advice and for being always accessible when I needed help.

To my current and alumni labmates and friends, Atin, Geetha, Majo, Elif, Ying, Fred, Seba, Kasia, Ye, Serdar, a huge THANKS!, for making such a great environment to work, and for their constant support.

To the people who made my settling in this country and this University a fun and extremely social experience: Pascal, Fede, Fabien, Seba.

To my friends, for the fun times out of the lab, and for being there to listen and to support me: Geetha, Majo, Fede, Chummu.

To my parents, sister and brothers, for being an inspiration for strength and tenacity, and for supporting me no matter what in this adventure.

To James, for the great times we enjoyed together and for being a key support during these last six months.

To the many people I met during this years and made my experience in this country diverse and exciting.

To all of you, THANKS!

Ana.

INTRODUCTION

Heavy metal homeostasis in plants

The mineral nutrition of higher plants is of fundamental importance to agriculture and human health. Amongst the minerals required by plants, heavy metal ions such as Cu^{2+}, Zn^{2+}, Mn^{2+}, Fe^{2+}, Ni^{2+} and Co^{2+}, are essential micronutrients, while other heavy metals like Cd^{2+}, Pb^{2+} or Hg^{2+} are nonessential and highly toxic for the cell (Clemens, 2001). For example, Cu^{2+} is a vital component for electron-transfer reactions mediated by proteins such as superoxide dismutase, cytochrome *c* oxidase and plastocyanin, while Zn^{2+} serves as a cofactor for many enzymes. Inside cells, metal concentration is tightly regulated, and typically metals remain bound to metal-containing molecules to avoid the detrimental effects that they could cause if present in a free form; formation of hazardous free radicals that could damage DNA or plasma membrane structure, for example (Hall, 2002; Marschner, 1995; Outten & O'Halloran, 2001; Rae *et al*., 1999; Williams *et al.*, 2000). Little is known about the mechanisms that govern metal ion concentrations in plants. However, the identities of some components have been determined, unveiling a complex set of peptides, proteins, transporters and organic molecules important for metal homeostasis and regulation in plants.

Chelators and chaperones

Chelators contribute to metal detoxification by buffering cytosolic metal concentrations. In plants, metal chelators include phytochelatins, metallothioneins, organic and amino acids.

Phytochelatins (PC) are small, enzymatically synthesized peptides that present the general structure $(\gamma\text{-Glu-Cys})_n\text{-Gly}$ (n=2-11) (Cobbett, 2000). PCs are rapidly induced *in vivo* by

a wide range of heavy metal ions, although it only has been shown that Cd^{2+} positively regulates PC synthase (Ortiz *et al*., 1995).

Metallothioneins (MTs) are ubiquitous, small proteins, which bind metal ions by metal-thiolate clusters (Hamer, 1986). MTs, unlike PCs, are gene-encoded proteins, and are involved in copper detoxification, cytosolic zinc buffering and scavenging of metals during leaf senescence (Garcia-Hernandez *et al.*, 1998; Rauser, 1999; Robinson *et al.*, 1996). Depending on the plant species, the effect of metals on the expression of MTs varies. In *Arabidopsis*, the transcription of MTs is enhanced by various metals (Murphy & Taiz, 1995).

Carboxylic and amino acids represent potential ligands for metals due to the reactivity of metals with S, N and O. To date, these chelators have been linked to metal translocation through the plant vascular system, although they could also interact with metals inside the cell. Citrate, for example, has been hypothesized to be a Cd^{2+} ligand, to form complexes with Ni^{2+} in Ni-hyperaccumulating plants, and to contribute to Zn^{2+} accumulation and tolerance. Nicotianamine is a non-proteinaceous amino acid, which chelates Fe^{2+} and other divalent cations as well as Fe^{3+} (Clemens, 2001).

Chaperones are peptides that deliver metal ions to metal-requiring proteins. Most of the current knowledge on these proteins has been obtained by studying copper chaperones and their target proteins inside the cell. In yeast, the copper chaperone ATX1 interacts and delivers copper to the Cu^{+}-ATPase CCC2 (Lin *et al*., 1997). The ATPase CCC2 is located in a post-Golgi compartment (Pufahl *et al*., 1997), and upon interaction with ATX1, copper is transported by CCC2 inside the lumen of a post-Golgi vesicle. Copper is then inserted into copper requiring proteins as they make their way to their specific intracellular targets (Lin *et al*., 1997). In humans, a homologue of ATX1, the copper chaperone HAH1, was cloned and shown to interact

with the Menkes disease protein (MNK) (Hamza *et al*., 1999). MNK is a Cu^{+}-ATPase, and mutations in this protein produce copper deficiency symptoms in humans (Lutsenko & Petris, 2002). CCH, a copper chaperone from *Arabidopsis* that presented homology to ATX1 has been cloned. It was observed that CCH is upregulated in senescent leaves (Himelblau *et al*., 1998). The presence of four putative Cu^{+} transporting ATPases in *Arabidopsis* suggest that in plant cells a Cu^{+} trafficking network analogous to the ones described in yeast and humans might exist.

Transporters

A number of transporters have been reported to have a role in metal transport through the plasma membrane, translocation through vesicular membranes and tonoplast or insertion into chloroplast and mitochondria. These transporters belong to the ZIP, NRAMP and CDF protein families, and to the heavy metal transport ATPases subfamily, also known as P_{1B}-ATPases. This subfamily of proteins uses the energy of ATP to transport metals against their concentration gradients.

The ZIP (ZRT, IRT-like Protein) family of transporters has been shown to be responsible for the transport of Fe^{2+} and Zn^{2+} ions. *Arabidopsis* sequence indicates the presence of 15 putative ZIP members (Maser *et al*., 2001). IRT1 and IRT2 are ZIP members thought to transport Fe^{2+}, and their transcription is induced in roots after iron starvation (Eide *et al*., 1996; Korshunova *et al*., 1999). Additional studies showed that IRT1 also transports Mn^{2+}, Zn^{2+} and Cd^{2+} (Cohen *et al*., 1998; Korshunova *et al*., 1999; Vert *et al*., 2001). *Arabidopsis* ZIP transporters 1-3 confer Zn^{2+} uptake activity when expressed in yeast cells and their transcripts are induced under Zn^{2+} starvation conditions (Grotz *et al*., 1998). A role for ZIP members in Zn^{2+} accumulation in hyperaccumulating species has also been proposed (Pence *et al*., 2000).

NRAMP (Natural Resistance-Associated Macrophage Protein) is a family of proteins that is also involved in the transport of heavy metal ions. The sequence of *Arabidopsis* genome revealed six genes encoding proteins with high homology to NRAMP genes. AtNRAMP1, 3 and 4 complement a yeast strain deficient in Mn^{2+} and Fe^{2+} uptake, and their expression increase its sensitivity to Cd^{2+} and its content inside yeast cells (Thomine *et al*., 2000). Moreover, overexpression of NRAMP1 in plants decreases iron sensitivity, thereby suggesting a role in intracellular sequestering (Curie *et al*., 2000).

The CDF (Cation Diffusion Facilitator) protein family has also been involved in heavy metal transport. Members of this family present six putative transmembrane domains plus a signature sequence in the N terminus (Paulsen & Saier, 1997). ZAT1 is an *Arabidopsis* CDF that transports Zn^{2+} (Bloss *et al.*, 2002; van der Zaal *et al*., 1999). A search of the complete *Arabidopsis* genome revealed the existence of eight genes encoding for CDF family members, although their specific role in metal transport is still to be elucidated (Maser *et al*., 2001).

Other proteins are related to metal homeostasis but appear not belong to any of the mentioned families. The *Arabidopsis* COPT1 transporter shows significant homology with a yeast copper uptake transporter, CTR1. Expression of COPT1 in yeast restores growth of *Δctr1-3* mutant strain, with a concomitant increase of sensitivity to high copper concentrations (Kampfenkel *et al*., 1995). The ABC-ATPases are involved in the efflux of many substrates using ATP as energy donor. In plants, ABC-type proteins are involved in the transport of plant toxins, Cd^{2+} (Li *et al*., 2002), Fe^{2+} (Rogers & Guerinot, 2002) and phytochelatin-Cd^{2+} complexes (Ortiz *et al*., 1995).

P_{1B}-ATPases

Heavy metal ATPases have been implicated in the transport of heavy metals across cell membranes (Axelsen & Palmgren, 1998; Lutsenko & Kaplan, 1995), typically by catalyzing metal export from cytoplasm to either extracellular space or intracellular compartments (Argüello, 2003). Heavy metal ATPases belong to the P-type family of ATPases, which are primary transporters that couple hydrolysis of ATP to ion translocation. P-type ATPases transport cations against their concentration gradients, and transport can be in one direction (one cation is being transported, e.g. Ca^{2+}-ATPase, H^+-ATPases) or in both directions (interchange of cations, e.g Na^+/K^+ ATPase, H^+/K^+ ATPase). Most P-type ATPases have a single subunit with eight to twelve transmembrane segments, N- and C-termini exposed to the cytoplasm, and a large central cytoplasmic domain including phosphorylation and ATP binding sites (Axelsen & Palmgren, 2001; Lutsenko & Kaplan, 1995). P-type ATPases form a phosphorylated intermediate during their catalytic cycle, and are inhibited by vanadate. The P-type ATPase family was subdivided into subfamilies based on sequence and functional similarities. Subfamily 1B comprises heavy metal ATPases, like the Cu^+-ATPases from Wilson and Menkes diseases, 2C/D includes the highly characterized Na^+/K^+ ATPase in animals, subfamily 3A contains the H^+-ATPases in fungi and plants and subfamily 2A/B comprises the Ca^{2+}-ATPases (Axelsen & Palmgren, 1998). During their catalytic cycle, all P-type ATPases adopt two conformations, E1 and E2, upon cation binding. Figure 1 shows the catalytic cycle for a typical P_{1B}-ATPase, which is analogous to all P-type ATPases that drive the outward movement of cations.

P_{1B}-ATPases contain 6 to 8 transmembrane fragments, as shown by hydrophobicity analysis (Fig 2). The topology of CadA from *H. pylori* (Melchers *et al*., 1996) and CadA from *S. aureus* (Tsai *et al*., 2002) has been experimentally determined, showing the presence of eight

transmembrane fragments. P_{1B}-ATPases also share the common feature of a conserved CPC, CPH, CPS, SPC or TPC motif in the transmembrane fragment six, which could be involved in metal ion binding and transport (Argüello, 2003). Experimental evidence indicates the Cys present in those domains in essential for enzyme function. Mutation in the Cys from CPC from CopA of *A. fulgidus* produces a loss of ATPase activity (Mandal & Argüello, 2003), and similar results were observed when Cys were mutated in CPC sequences of *C. elegans* Cu-ATPase (Yoshimizu *et al*., 1998), in *E. hirae* CopB (Bissig *et al*., 2001) and *E. coli* CopA (Fan, 2002).

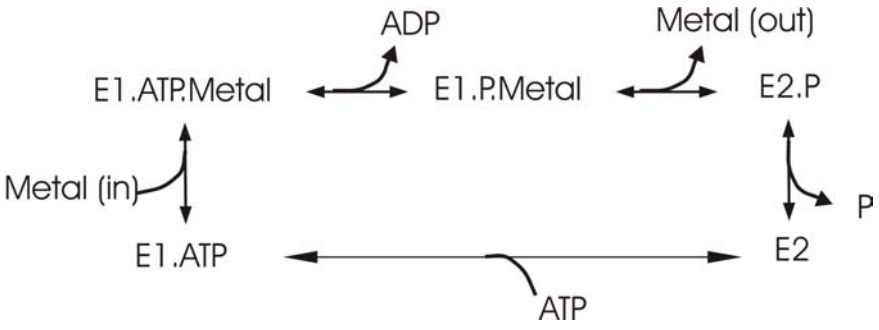

Figure 1: Catalytic cycle of a model P_{1B}-ATPase. Binding of ATP produces a conformational change from E2 to E1, which allow binding of the metal ion from the cytoplasmic side. This is followed by phosphorylation of a conserved aspartate residue in the protein, and the release of the metal ion on the other side (either extracellular or intracellular compartments) provokes a conformational change to E2, with subsequent dephosphorylation.

Many of these enzymes also present a cytoplasmic metal binding domain in the N terminus (Fig 2), that consists of a conserved CXXC sequence or a His stretch (Argüello, 2003). The two human Cu^+-ATPases, the Wilson and Menkes disease proteins, contain six CXXC sequences in the N terminus, and copper binds with a stoichiometry of one copper atom per metal-binding repeat (Lutsenko *et al*., 1997). Other examples are CadA from *Listeria monocytogenes,* which transports Cd^{2+} and contains one CXXC repeat (Mitra & Sharma, 2001)

and ZntA from *E. coli* also contains one CXXC motif (Rensing *et al.*, 1997). Additionally, proteins with His rich motifs include *E. hirae* CopB (Odermatt *et al*., 1993) and CopB from *A. fulgidus* (Mana-Capelli *et al*., 2003).

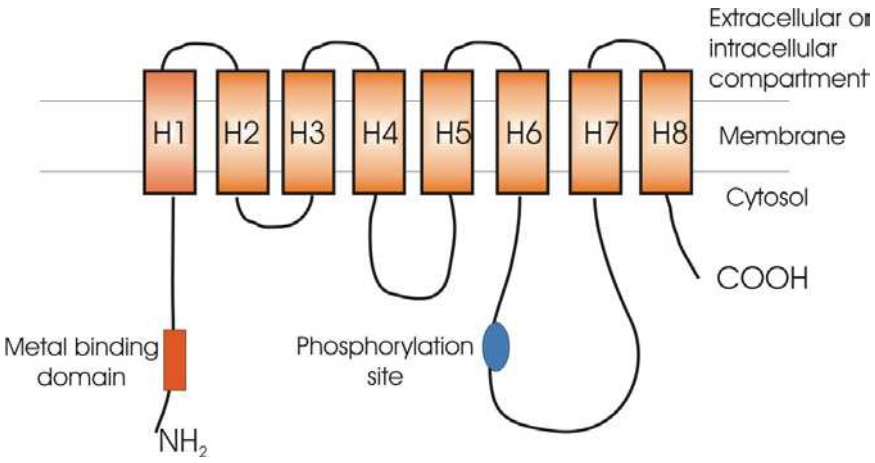

Figure 2: Scheme of a typical P_{1B}-ATPase. These ATPases present eight transmembrane fragments (H1 to H8), with a conserved CPC, CPH or CPS in H6. The metal binding domain consists of a consensus sequence CXXC or a His repeat stretch; phosphorylation of the aspartate in the conserved sequence DKTGT occurs during catalytic cycle.

Originally, the N terminal metal binding domain was thought to participate in metal binding and transport. The role of the metal binding domain was further explored, and it was shown it is not essential for enzymatic activity; either removal of this domain or point mutations in the Cys of the CXXC consensus sequence did not suppress completely protein activity. Therefore, this domain was proposed to be regulatory (Mana-Capelli *et al*., 2003; Mandal & Argüello, 2003; Mitra & Sharma, 2001; Voskoboinik *et al*., 2001; Voskoboinik *et al*., 1999).

Metal specificities of P_{1B}-ATPases

One striking feature about P_{1B}-ATPases is that, while sharing similar consensus sequences, their specificities towards metal ions differ greatly. Therefore, it is apparent that the specificity determinants lie somewhere else in the protein structure. Based on sequence homology and similarity to functionally characterized P_{1B}-ATPases, these enzymes were subdivided in five groups, IB1-5 (Argüello, 2003). Each subgroup presents a characteristic N terminal metal binding domain (N-MBD), a typical sequence in H6 plus signature sequences in H7 and H8, associated with their metal specificities. The structural characteristics of each subgroup are summarized in table 1.

Subgroup	Metal specificity	N-MBD	H6	H7	H8
1B-1	Cu^+/Ag^+	0-6 CXXC	CPC	NX_6YNX_4P	$MX2SSX_5[N/S]$
1B-2	$Zn^{2+}/Cd^{2+}/Pb^{2+}$	0-2 CXXC + $(HX)_n$	CPC	NX_7K	$DXGX_7N$
1B-3	$Cu^{2+}/Cu^+/Ag^+$	H-rich	CPH	NX_5GYNX_4P	$PXMSXSTX_5N$
1B-4	Co^{2+}	-	SPC (H4)	not-identified	$HEG[G/S]TX_5[N/S][G/A/S]$
1B-5	?	-	TPC	not-identified	not-identified

Table 1: Structural characteristics of each subgroup in the P_{1B}-ATPase subfamily. Metal specificity and type of N terminus metal binding domain are shown, together with consensus sequences in H6 (in H4 for 1B-4 members) and signature sequences in H7 and H8 (in H6 for 1B-4 members).

Proteins belonging to subgroup IB-1 transport Cu^+ and are also activated by Ag^+ but not by divalent ions. Examples of these proteins are found in the Menkes and Wilson disease proteins (Bull & Cox, 1994; Bull *et al*., 1993; Petrukhin *et al*., 1994; Vulpe *et al*., 1993), *A. thaliana* HMA6 and HMA7 (previously named PAA1 and RAN1, respectively) (Hirayama *et al*.,

1999; Shikanai *et al.*, 2003; Tabata *et al*., 1997; Woeste & Kieber, 2000), *E. coli* CopA (Rensing 2000), the yeast Cu^{+}-ATPase CCC2 (Pufahl *et al*., 1997) and *A. fulgidus* CopA (Mandal *et al.*, 2002). Subgroup 1B-2 includes $Zn^{2+}/Cd^{2+}/Pb^{2+}$ transporters. Members of this group are found in archaea, prokaryotes and plants, being the latter the only eukaryotes were these proteins are found. Proteins belonging to this subgroup include *E. coli* ZntA (Rensing *et al*., 1997; Sharma *et al*., 2000), *H. pylori* CadA and HMA2, the first Zn^{2+}ATPase functionally characterized in eukaryotic organisms (Eren & Argüello, submitted for publication). Proteins belonging to subgroup 1B-3 include only prokaryotic members. These proteins transport Cu^{2+}, Cu^{+} and Ag^{+}, the former at a higher rate than the latter (Mana-Capelli *et al*., 2003). Examples of these proteins can be found in CopB from *A. fulgidus* (Mana-Capelli *et al*., 2003) and CopB from *E. hirae* (Odermatt *et al*., 1993).

Subgroup 1B-4 contains P_{1B}-ATPases with a total of six transmembrane fragments compared to the eight that characterizes this subfamily of proteins. Metal specificity was determined experimentally for only one member of this subgroup, CoaT from *Synechocystis* PCC6803. Disruption of CoaT gene leads to Co^{2+} sensitivity and accumulation, therefore indicating a role in Co^{2+} transport (Rutherford *et al.*, 1999). In this subgroup, the consensus sequence usually found in H6, is present in H4, the functional equivalent of H6, and it is SPC, with no signature sequence identified in H5. Another protein belonging to this group is HMA1 from *A. thaliana*, one of the targets of this study. Subgroups 1B-5 and 1B-6 include the remainder of the proteins that could not be included in any of the mentioned groups. Their specificity determinants are still to be found (Argüello, 2003).

P_{1B}-ATPases in Arabidopsis

Arabidopsis thaliana contains eight P_{1B}-ATPases, named HMA1-8, and together with *Oryza sativa*, comprises the highest number of P_{1B}-ATPases found in a single organism (Argüello, 2003; Axelsen & Palmgren, 2001; Baxter *et al.*, 2003). Phylogenetic analysis of their sequences, show that HMA2-4 are closely related, HMA5-8 cluster together and HMA1 is more distantly related to the other two groups (Axelsen & Palmgren, 2001; Baxter *et al.*, 2003; Cobbett *et al.*, 2003; Williams *et al*., 2000). Based on Argüello's classification in functional subgroups, HMA1 belongs to the 1B-4 subgroup, HMA2-4 to the 1B-2 and HMA5-8 to the 1B-1 subgroup. Moreover, among eukaryotic organisms, only plants contain members of subgroups 1B-2 and 1B-4, as humans and yeast present P_{1B}-ATPases only belonging to subgroup 1B-1 (Argüello, 2003).

The first P_{1B}-ATPase reported in higher plants was HMA6 from *Arabidopsis thaliana* (Tabata *et al*., 1997). No variation in HMA6 expression was observed when *Arabidopsis thaliana* plants were grown in different $CuSO_4$ concentrations. Furthermore, no functional data supporting a role in metal transport was provided. Recently, mutant plants in HMA6 gene that presented a high chlorophyll fluorescence phenotype were isolated (Shikanai *et al.*, 2003). These mutants were defective in photosynthetic electron transport, exhibited less concentrations of copper-bound plastocyanin, a chloroplastic protein, and lower activity of other chloroplastic proteins compared to wild type plants. Mutant plants also contained lower Cu^{2+} content in chloroplasts, and the mutant phenotype was recovered upon Cu^{2+} treatment. This experimental evidence suggests that HMA6 pumps copper into the chloroplast. Functional evidence has also been provided for the role of HMA7 in Cu^{+} transport. The HMA7 gene was identified when plants were screened for constitutive ethylene response in the presence of a potent ethylene

antagonist, TCO. The expression of HMA7 gene complemented growth of yeast mutant for the CCC2 Cu^{+}-ATPase, therefore indicating a role in Cu^{+} transport. Based in this evidence, it was proposed that HMA7 might act delivering Cu^{+} in the trans Golgi for the assembly of functional ethylene receptors (Hirayama *et al*., 1999). In a later work, the essential role of HMA7 for plant metabolism was shown as mutant plants exhibited a rosette-lethal phenotype when grown in soil, and smaller and unfertile plants when grown in Gamborg's media (Woeste & Kieber, 2000).

HMA4 was the first protein from subgroup 1B-2 to be reported (Mills *et al*., 2003). Expression of HMA4 complemented growth of *ΔzntA E.coli* in high Zn^{2+} media. HMA4 also confers resistance to Cd^{2+} when expressed in the mutant *Saccaromyces cerevisiae* strain *Δycf1*. This evidence suggests that HMA4 transports Zn^{2+}/Cd^{2+}, consistent with its placement in subgroup 1B-2. HMA4 transcript is also found in all plant organs, except for siliques, and it increases upon Zn^{2+}, Cd^{2+} and Ni^{2+} treatment and decreases upon Mn^{2+} treatment (Mills *et al*., 2003; Orofino & Argüello, unpublished results). A recent publication provides evidence that HMA3 might be involved in Cd^{2+} and Pb^{2+} transport to intracellular compartments, as its expression complemented strain *Δycf1* when grown in high Cd^{2+} or Pb^{2+} containing-media (Gravot *et al.*, 2004). Biochemical evidence of Zn^{2+} and Cd^{2+} transport has been provided for HMA2 (Eren & Argüello, submitted for publication). HMA2 transports Zn^{2+} and Cd^{2+} with high affinity, and other metals to a lesser extent. As a typical P-type ATPase, HMA2 forms a stable phosphorylated intermediate and it is inhibited by vanadate. Metal transport experiments evidence that HMA2 drives the outward movement of metals from the cytoplasm to the extracellular milieu. HMA2 transcript is present in all plant organs and does not change upon metal exposure. Under normal grown conditions, mutant plants for HMA2 gene present higher Zn^{2+} concentration, and further Zn^{2+} accumulation if grown in Zn^{2+} containing media. When

exposed to high Cd^{2+} concentrations, mutant plants accumulate this metal to a higher extent than wild type plants, further supporting a role in Zn^{2+} and Cd^{2+} transport (Eren & Argüello, submitted for publication).

Functional evidence for HMA1, HMA5 and HMA8 metal transport has not yet been provided. Results obtained in our laboratory indicate that HMA5 transcript is found only in roots and is upregulated in high Cu^{2+} media; HMA8 transcript in found in all plant organs, and also upregulated in high Cu^{2+} media (Eren, Orofino & Argüello, unpublished results).

The high number of P_{1B}-ATPases found in *Arabidopsis*, and the distinct expression patterns found in members belonging to the same functional subgroup, indicates different transport processes in different compartments of the plant body. Where these proteins are expressed in the whole plant provides information on the roles they may play in metal homeostasis. Changes in expression upon metal stress or deficiency may indicate if they are also related to metal tolerance mechanisms. Moreover, the effect of P_{1B}-ATPase gene mutation in plant metabolism might provide insight on how essential these genes are for integral plant physiology. In this work, two P_{1B}-ATPases from *Arabidopsis thaliana*, HMA1 and HMA6 were chosen for study. The goals of this work were to clone and sequence these genes for functional studies, to determine their mRNA-transcript levels in different plant organs and in seedlings grown at different metal concentrations, and to determine the effect of T-DNA insertions in these genes in plant growth and development.

MATERIALS AND METHODS

Plant material. Seeds of *Arabidopsis thaliana* ecotype Columbia 0 (Col0) were grown in soil or in growth media at 23ºC with a photoperiod 14 hours light:10 hours dark. For metal tolerance experiments, seeds from *Arabidopsis thaliana* ecotype Col0 were surface-sterilized by submerging them in 70 % ethanol for 2 min, 10 min in 20 % bleach, 0.2 % SDS and washed ten times with sterile water. Sterile seeds were placed in plates containing Murashige-Skoog (MS) Salt Mixture media with vitamins (Invitrogen Co, Carlsbad, CA) with 1% agar plus addition of different metal concentrations, stratified at 4°C for two days and grown at the same photoperiod and temperature stated before. For seedling growth determination, the metals and final concentrations tested were 0, 0.1, 0.25 and 0.5 mM of $CuSO_4$, $ZnSO_4$, $CdCl_2$, $NiSO_4$, $CoCl_2$, $FeSO_4$, $MnCl_2$ and $AgNO_3$. For root length measurements, excess metal media was prepared by mixing MS media with each metal to final concentrations of 0.1 mM $CuSO_4$, 0.25 mM $ZnSO_4$, 0.25 mM $CdCl_2$, 0.25 mM $NiSO_4$, 0.25 mM $CoCl_2$, 0.5 mM $MnCl_2$ or 0.1 mM $AgNO_3$. Metal deficient media was prepared by mixing all MS media components except for the metal salt for which deficiency was tested.

Cloning in pBADTOPO vector and expression in bacteria. DNA sequences for HMA1 and HMA6 genes were obtained through GenBank (http://www.ncbi.nlm.nih.gov/). Leaves from 4 week-old plants were harvested, frozen in liquid N_2 and kept at -80ºC for RNA extraction. Approximately 100 mg of frozen leaf tissue from 4 week-old Col0 plants was grinded in liquid N_2, and total RNA was extracted using the RNeasy Plant mini kit (QIAGEN Inc, Valencia, CA) following the manufacturer's specifications. RNA integrity was analyzed in formaldehyde agarose-gels (Sambrook *et al.*, 1989). Single stranded cDNA was synthesized using Superscript

II-H$^-$ Reverse Transcriptase (Invitrogen Co, Carlsbad, CA) following the manufacturer's protocol. 2 μg of total RNA was used per 20 μl of RT reaction final volume.

For PCR amplification of coding sequence of HMA1 gene, primers used were 5HMA1 and 3HMA1; for HMA6 gene, primers 5PAA1 and 3PAA103 were used (Table 2). For HMA1 gene, a stop codon was included given that HMA1 contains a six His residues in tandem at its N terminal. The positive control for the polymerase function consisted in two primers specific for the flanking sequence of a clone of known size (~200pb). The PCR program consisted in 95° 2 min, 15 cycles of 95° 15 sec, 60° 30 sec, 68° 8 min, and then 25 cycles of 95° 15 sec, 60° 30 sec, 68° 8 min plus 20 seconds per cycle. Expand Polymerase (Roche) was used, which exhibits good proofreading activity and, like Taq Polymerase, adds an A overhang in the 3' end. PCR fragments were analyzed in 1% agarose gels containing 0.5 μg/ml Ethidium bromide (Sambrook *et al*., 1989). Amplified fragments were cloned in pBAD-TOPO vector (Invitrogen Co, Carlsbad, CA) following manufacturer's protocol.

The DNA sequence of HMA1 and HMA6 was confirmed by automated DNA sequence analysis (Davis, Keck and Macrogen facilities) with the primers listed on Table 2.

For expression in bacteria, *E. coli* strains used were TOP10, TOP10 CP, BL21 DE3(pLys)S, BL21 DE3(pLys)SStar and BL21 AI (Invitrogen). All protein concentration determinations were performed using the Bradford reagent (Bradford, 1976). An aliquot of an overnight culture of transformed cells was inoculated in 25 ml 2xYT media plus addition of 100 μg/ml Ampicillin, or plus 100 μg/ml Ampicillin and 34 μg/ml Chloramphenicol for BL21 cells. These cultures were grown at 37°C or 22°C until $O.D._{600}$ of 0.6 (exponential phase of growth), at which arabinose was added to a final concentration of 0.002 % to induce expression. After three hours, 1 ml aliquots of culture were taken; cells were spun and lysed by sonication.

HMA1 gene				
5' PRIMERS				
Primer name	**Position in ORF**	**Position in gene**	**Comments**	**Use in this work**
5HMA1	4-32	4-32	-	Cloning-Sequence-T-DNA
5HMA102	334-357	334-357	-	Sequence
5HMA103	1330-1365	2264-2299	D→A (NheI site)[a]	Sequence
5HMA104	-	3691-3715	Intron localized	T-DNA screening
Y5HMA1	1-20	1-20	SacI + AATA[b]	Cloning in pYES
3' PRIMERS				
3HMA1	2431-2460	4338-4366	Stop codon [c]	Cloning-Sequence
3HMA102	2251-2271	4069-4092	-	Sequence
3HMA103	1337-1364	2264-2299	D→A (NheI site)[a]	Sequence
3HMA104	228-252	228-252	-	T-DNA screening
3HMA105	-	3973-3998	-	T-DNA screening
Y3HMA102	2439-2447	4345-4363	NotI site[d]	Cloning in pYES
HMA6 gene				
5' PRIMERS				
Primer name	**Position in ORF**	**Position in gene**	**Comments**	**Use in this work**
5PAA1	1-30	1-30	-	Cloning-Sequencing
51PAA102	473-496	559-582	-	Sequencing
51PAA103	1645-1651	4295-4318	Last 16bp intron[e]	Sequencing
5PAA104	-	1332-1361	Intron localized	T-DNA screening
5PAA105	1-3	-57-3	5'UTR	T-DNA screening
5PAA106	-	-557-(-536)	5'UTR	T-DNA screening
Y5PAA1	1-20	1-20	KpnI site +AATA[b]	Cloning in pYES
3' PRIMERS				
3PAA1	2822-2850	6829-6857	Stop codon[c]	Sequencing
3PAA102	2264-2286	5597-5619	-	Sequencing
3PAA103	2818-2847	6825-6854	Plus 15bp EK site[f]	Cloning
3PAA104	2489-2511	6088-6110	-	Sequencing
3PAA105	486-511	555-579	CGGC→AGGA (NaeI)[a]	Sequencing
3PAA106	1668-1695	3721-3748	CPC→APA (NotI)[a]	Sequencing
3PAA107	-	1521-1549	Intron localized	T-DNA screening
3PAA108	334-354	334-354	-	T-DNA screening
Y31PAA1	2829-2847	6840-6854	NotI site[d]	Cloning in pYES

Table 2 legend on next page

Table 2: Primers for HMA1 and HMA6 genes used in this work.

[a] Primer includes a point mutation plus adding a restriction site.

[b] Forward primers for cloning in pYES vector. Restriction site plus AATA sequence added for transcription in yeast.

[c] Stop codon was included in the reverse primer used to amplify the complete ORF.

[d] Reverse primer for cloning in pYES adds a restriction site.

[e] First 6 bp anneal to exon and remaining 16 bp to intron.

[f] Reverse primer adds sequence for digestion with Enterokinase to eliminate C terminus $(His)_6$ tag.

Protein concentration was determined, and equal concentrations of protein were loaded in polyacrylamide gels for SDS-PAGE (Laemmli, 1970). Gels were stained with Coomasie Brilliant Blue or blotted onto nitrocellulose membranes, and developed with Anti-His antibody as primary antibody, and anti-rabbit IgG, Horseradish Peroxidase-conjugated secondary antibody. For metal tolerance assays in bacteria, *E.coli* TOP10 cells transformed with HMA6-pBADTOPO and HMA1-pBADTOPO were induced for protein expression for 90 min, and diluted 1:20 in 2xYT media plus addition of 50 and 75 μM $AgNO_3$, 4 and 6 mM $CuSO_4$, 1 and 1.5 mM $ZnSO_4$, 0.5 and 1 mM $CdCl_2$, 1 and 1.5 mM $CoCl_2$ and 2 and 3 mM $NiSO_4$, and grown for 3 h. *ΔcopA* strain (parental LMG194) was transformed with HMA6-pBADTOPO. After 2h expression, complementation was assayed by diluting cultures 1:20 in 2xYT media supplemented with 1 mM, 2 mM or 3 mM $CuSO_4$, and growing them for 6 h.

Cloning In Yeast Expression Vector and Expression. HMA1 cDNA was subcloned into the SacI and NotI sites, and HMA6 into the KpnI and NotI sites of the yeast expression vector pYES2/CT (Invitrogen Co, Carlsbad, CA) under the control of the *GAL1* promoter. Yeast strain INVSc1 MATα his3Δ1 leu2 trp1-289 ura3-52 (Invitrogen) was transformed with HMA1-pYES, HMA6-pYES or pYES alone by electroporation. Transformants were selected in uracil-depleted SD media (6.7g.l^{-1} yeast nitrogen base, 1.92 g.l^{-1} yeast synthetic drop-out media without uracil

(Sigma)) supplemented with 20 $g.l^{-1}$ glucose. To induce HMA1 or HMA6 expression, cells were diluted to $O.D._{600}$ 0.6 in the same media containing 20 $g.l^{-1}$ galactose and grown for 8 h. For complementation assays, different yeast strains were transformed with the same constructs. Two *Δccc2* mutant strains were transformed with HMA6-pYES and pYES vectors, parental strain 2809 (MATα his3-200 leu2 trp1-101 ura-52 ade5) (kindly provided by Dr. Andrew Dancis, University of Pennsylvania) and BY4743 (MAT a/α his3Δ1/ his3Δ1 leu2Δ0/leu2Δ0 lys2Δ0/LYS2 MET15/met15Δ0 ura3Δ0/ ura3Δ0) (Invitrogen). *Δfet3* in the background BY4743 (Openbiosystems) was also transformed with HMA6-pYES and pYES vectors. *Δycf1* (Invitrogen) and *Δcot1* (Openbiosystems) in the BY4743 background were transformed with HMA1-pYES or pYES vectors.

Complementation assays in yeast. One fresh yeast colony was grown overnight in uracil depleted SD media with 20 $g.l^{-1}$ glucose and diluted 1:10 the next day. Yeast cells were grown until $O.D._{600}$ of 0.6, diluted in the same media but supplemented with 20 $g.l^{-1}$ galactose and grown for 4 h to allow protein expression. At that time, 1 ml of a culture with $O.D._{600}$ 0.8 was spun down, and pellet resupended in 100 µl SD media. 1:10 serial dilutions were made and 5 µl were spotted in SD media supplemented with 20 $g.l^{-1}$ galactose and 10 $g.l^{-1}$ raffinose (2809 strain) or 20 $g.l^{-1}$ galactose (BY4743 strain) plus 1% agar. For growth of the mutant strains in the BY4743 background, 200 µg/ml of Geneticin was added to the media. For complementation of *Δccc2* in the 2809 background, 60 µM Bathophenanthroline disulfonic acid (BSDS) and 60 µM Bathocuproine disulfonate (BCS) were added to the solid media, for *Δccc2* strain BY4743, 30 µM BSDS or 300 µM BCS were added to the solid media. Complementation of *Δfet3* strain was tested in media plus addition of 0.5 mM to 4 mM $CuSO_4$. *Δycf1* and *Δcot1* (BY4743) were transformed with HMA1-pYES but no expression was detected up to 24 h post induction.

***E. coli* and yeast membrane preparation.** Membrane fractions of *E. coli* cells were prepared according to Mandal *et al* (2002) with some variations. Briefly, cells were washed with 25 mM Tris-HCl, 100 mM KCl buffer pH 7, weighed and stored at -80°C. The cells were resuspended in Buffer A (25 mM Tris-HCl pH 7.5, 100 mM sucrose) plus 1 mM phenylmethylsulfonyl fluoride (PMSF). The extracts were lysed using French Press 3 times at 20000 psi and incubated with 2 mM $MgCl_2$ and 0.02 mg/ml of DNAse I at 4°C 30 min. The cell lysate was diluted 1:1 in Buffer A plus 1 mM PMSF and spun at 27,000xg 30 min. The supernatant (cleared lysate) was centrifuged at 100,000 x g 1 h and the pellet (membrane fraction) was washed 1 h in buffer A plus 1 mM PMSF, resuspended in buffer A plus 1 mM PMSF, total protein concentration was determined by Bradford method and approximately 10 mg protein aliquots were stored at -20°C in 20 % glycerol.

Total membranes of yeast cells were prepared as described by Voskoboinik *et al* (2001) with some modifications. Briefly, cells were suspended in 25 mM Tris HCl (pH 7.4), 250 mM sucrose, 10 mM ascorbate, 1 mM PMSF, 1 $\mu g.ml^{-1}$ leupeptin and 1 $\mu g.ml^{-1}$ aprotinin. Cells were disrupted in a Beads Beater (BioSpec, Bartlesville, OK) 4 x 30 sec homogeneization with 30 sec intervals plus 1 min interval after each cycle. The homogenate was centrifuged at 10,000 x g for 20 min. The supernatant was centrifuged at 110,000 x g for 1 h and the pellet was resuspent in the same buffer described before but with 0.2 mM ascorbate instead.

ATPase activity assays. All phosphate determinations for assessing ATPase activity were performed as described by Mandal *et al*. (2002). The ATPase assay mix contained 50 mM Tris-HCl pH 7, 3 mM MgCl2 and 3 mM ATP in a final volume of 250 µl, with enzyme, metal and cofactor additions. All reactions were incubated at 37°C for 20 min. The reaction was stopped by placing tubes in ice. 750 µl of the color reagent (3 volumes of 0.045 % Malachite green and 1

volume of 4.2 % Ammonium Molybdate in 4 N HCl) was added, vortexed and the colorimetric reaction was stopped by addition of 100 µl of 34 % Sodium Citrate. The absorbance at 660 nm was recorded.

Phosphorylation assays. Phosphorylation by ATP was assayed with 100 µg yeast membrane protein in buffer containing 50 mM Tris HCl pH 7.5, 1 mM $MgCl_2$, 50 mM NaCl, 5 µM [γ-^{32}P] ATP, 20% Dimethyl sulphoxide (DMSO) and addition of 10 and 100 µM $AgNO_3$ or 10 and 100 µM $CuSO_4$ plus 2.5 mM Dithiothreitol (DTT) in a 100 µl final volume. 5 mM EDTA was added to controls. The reactions were initiated by addition of [γ-^{32}P] ATP. After 60 sec incubation, phosphorylation was stopped by addition of five volumes of stopping solution (ice cold 10% trichloroacetic acid, 1 mM Na_2HPO_4). Samples were centrifuged 14,000 x g 10 min, pellets were washed with five volumes of stopping solution and centrifuged 14,000 x g 10 min. Pellets were resuspended in acidic loading buffer (5 mM Tris-PO_4, pH 5.8, 6.7 M urea, 0.4 M DTT, 5% SDS and 0.014% bromophenol blue) and resolved by SDS-PAGE in 8% acidic gels (Sarkadi *et al.*, 1986).

Transcript level determination by RT-PCR. RNA from seedlings growing in MS media plus 0.1 mM $CuSO_4$, 0.25mM $ZnSO_4$, 0.25 mM $CdCl_2$, 0.25mM $NiSO_4$, 0.25 mM $CoCl_2$, 0.5mM $MnCl_2$ and 0.1mM $AgNO_3$, and from roots, leaves, flowers and stems of 6 week-old plants was extracted using the RNeasy Plant Midi kit (QIAGEN Inc, Valencia, CA) following the manufacturer's specifications. RT reaction was done following manufacturer's protocols and PCR cycle consisted in 95° 2 min, x number of cycles of 95° 15 sec, 55° 30 sec, 72° 3 min, and a final elongation of 3 min at 72°C. Amplification of EF1α transcription factor was used as control. For amplification of EF1α from seedlings and organs, x equaled 25. For HMA1

amplification in seedlings, 30 cycles were used, and 25 cycles for organs. For HMA6 amplification in seedlings and organs, 30 cycles were used. For determination of HMA1 transcript in *hma1-1* mutant, and transcript levels of proteins involved in metal homeostasis, RNA was extracted from leaves of 6 weeks-old WT and *hma1-1* plants. The PCR program was the same than before, and the number of cycles for HMA3 and HMA4 genes was 30; for EF1α, MT1a, MT1b, PCS1 and PCS2 genes, 25 cycles; and for MT2a and MT2b genes, 20 cycles.

PCR screening T-DNA Insertion Plants. Seeds of Col0 ecotype and T-DNA insertion mutant lines (Alonso *et al.*, 2003) were grown in soil after two-day stratification at 4°C. The T-DNA insertion lines screened were, for HMA1 gene, SALK_088042 and 043265; for HMA6 gene, SALK_072581 and 109629 (Table 3). One leaf from each of 2 week-old plants was harvested and genomic DNA preparation was made according to Edwards *et al.* (1991). Briefly, the lid of an eppendorf tube was used to pinch out a leaf disc, the tissue was macerated with disposable grinders (Scienceware, NJ) 15 sec and 400 µl of extraction buffer was added (200 mM Tris HCl pH 7.5, 250 mM NaCl, 25 mM EDTA and 0.5 % SDS). The extract was centrifuged 13,000 x g 1 min in a microfuge, and 300 µl of the supernatant are added to 300 µl of room temperature isopropanol, left 2 min at room temperature and then spun at 13,000 x g for 5 min. The pellet was air-dried and resuspended in 50 µl 1x TE buffer. 2 µl of this preparation are used for PCR screening. The primers used for the screening of each line are shown in Table 3. The program used for PCR screening was 94°C 2 min, 30 cycles of 94°C 15 sec, 60°C 30 sec, and 72°C 2 min. The same program was used to amplify a 600 bp fragment from the T-DNA sequence, used as a control (with primers 5LBb1 and 3LBb2).

Gene	SALK insertion line	WT pair	Insertion pair
HMA1	088042	HMA1-3HMA104	5HMA1-3LBb1
HMA1	043265	5HMA104-3HMA105	3LBb1-3HMA105[a]
HMA6	072581	5PAA104-3PAA107	5PAA104-3LBb1
HMA6	109629	5PAA105-3PAA107	3LBb1-3PAA107[a]
HMA6	109629	5PAA106-3PAA108	3LBb1-3PAA108[a]

Table 3: T-DNA insertion lines and primer pairs used for screening of mutants. WT pair amplifies only if the insertion is not in the expected site; insertion pair amplifies if T-DNA is present at the expected position.

[a] Primer 3LBb1 was used as the forward primer since the T-DNA insertion was in the opposite direction

Chlorophyll and metal content determinations. Chlorophyll from WT and *hma1-1* plants was extracted according to Wu *et al* (2002) with some modifications. 0.1 to 0.2 gr of leaves were frozen in liquid N_2 and pulverized. 2 ml of ice-cold 80 % acetone was added per 0.15 g of leaves and left for 1 h on ice. Samples were centrifuged for 15 min at 5000 x g. A_{663} (Chlorophyll A) and A_{645} (Chlorophyll B) was measured and total Chlorophyll was calculated using the equation:

$$\mu g\ Chl/ml = 20.2 \times A_{663} + 8.02 \times A_{645}$$

For metal content measurements, approximately 700 mg of leaf samples were digested in 7 ml of 4.5 N HNO_3 at 80˚C for 4 h, and left overnight at room temperature. The next day, 0.5 ml of 30% H_2O_2 were added, samples were filtered in Wathman #1 filters, and diluted with water to 15 ml. Fe^{2+}, Zn^{2+}, Cd^{2+} and Mn^{2+} contents were analyzed by atomic absorption spectroscopy (Perkin Elmer AAnalyst 300). For metal content determination per dry weight, approximately 3 g of whole plant tissue was dried at 80ºC for 3 days, ashed at 480ºC for 16 h and digested with HNO_3 as described above.

RESULTS

HMA1 and HMA6: Predicted topology and metal specificity

The sequence of HMA1 and HMA6 indicates they are membrane bound proteins. Therefore, topological maps were constructed to localize which segments are inside the membrane, and which fragments are oriented to cytoplasm or extracellular milieu. The prediction of the membrane spanning regions was made using the TMHMM 2.0 prediction program (http://www.cbs.dtu.dk/services/TMHMM/) and topogical maps of HMA1 and HMA6 were constructed using the TOPO2 program (http://www.sacs.ucsf.edu/TOPO-run/wtopo.pl). HMA1 contains six transmembrane fragments (H1 to H6), while HMA6 contains eight (H1 to H8). HMA1 differs from the typical eight transmembrane fragments array found in most P_{1B}-ATPases. Topologically, HMA1 can be viewed as any other P_{1B}-ATPase with the exception of lacking the first two transmembrane fragments. Therefore, while HMA6 presents a CPC sequence in H6, HMA1 contains an SPC in H4, the functional equivalent of H6 (Fig 3). HMA1 presents a His stretch in the N terminus that could be involved in heavy metal binding, while HMA6 presents one CGGC sequence in the cytoplasmic N terminus. Both of them present a phosphorylation site, DKTGT, and the HP consensus sequence in the large cytoplasmic loop. HMA1 contains a mitochondria-targeting sequence in the N terminus, while HMA6 has a chloroplast signal peptide, thus indicating a possible localization to mitochondria and chloroplast, respectively.

Analysis of HMA1 and HMA6 sequences shows that they belong to subgroups 1B-4 and 1B-1, respectively (Argüello, 2003). Proteins that are apparently involved in Co^{2+} transport share the signature sequence H-E-G-[G/S]-T-X_5-[N/S]-[G/A/S] in H6. Cu^{+} and Ag^{+} transporters contain the sequence N-X_6-Y-N-X_4-I-P-X-A in H7 and M-X_2-S-S-X_5-N in H8.

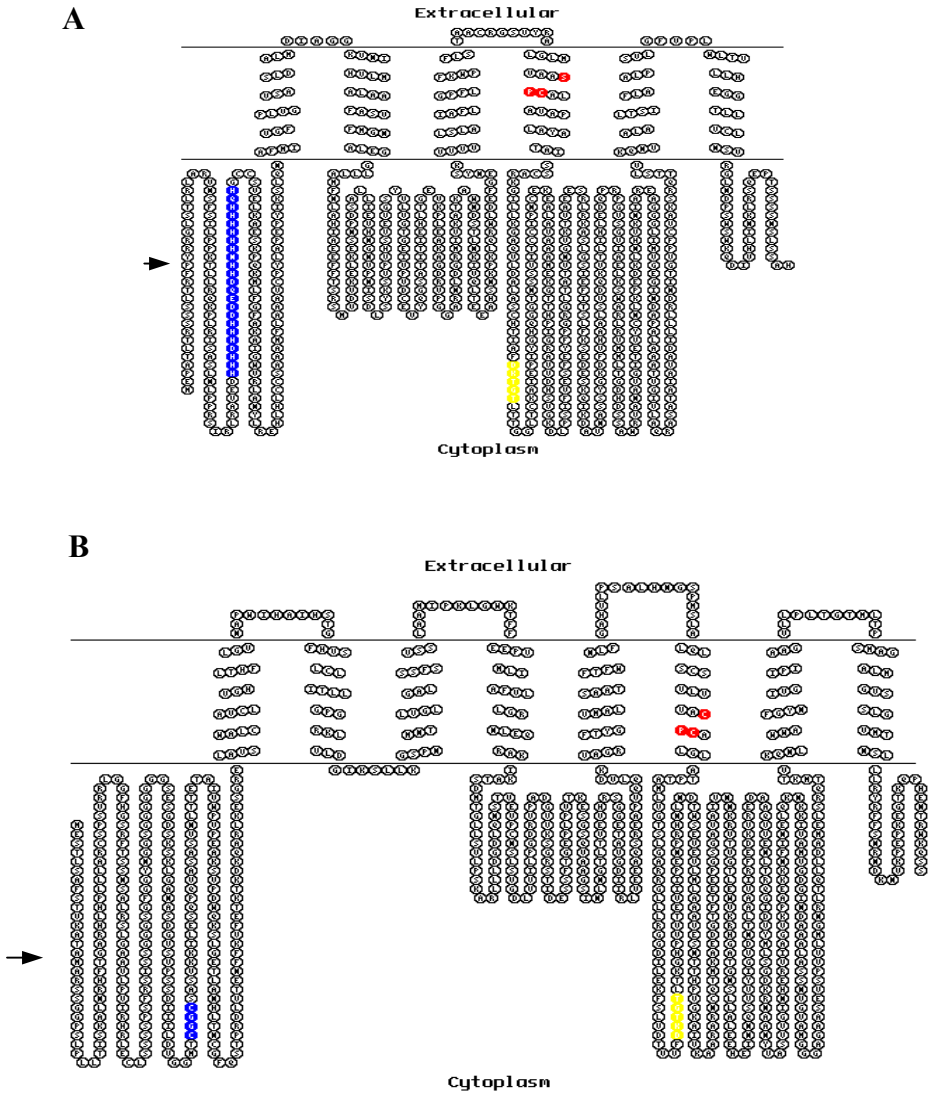

<u>Figure 3:</u> Topological maps of HMA1 and HMA6. For the two proteins, the phosphorylation site DKTGT in the large cytoplasmic loop is shown in yellow and the N-terminal binding domain in blue. In (A), map of HMA1, showing the six transmembrane fragments, a His stretch at the cytoplasmic N terminus (blue) and the SPC sequence in the H4 (red). In (B), sequence map of HMA6, showing one CGGC metal binding domain at the N terminus (blue) and the CPC sequence at the H6 (in red). In both, an arrow is indicating the transit peptide cleavage site, at amino acid 17 for HMA1 and amino acid 14 for HMA6, respectively.

HMA1 contains a signature sequence **HEGGT**LLVCLN**S** in H6, as it is shown in Figure 4, and as CoaT from *Synechocystis* PCC6803. HMA6 contains a **N**LWWAFG**YN**IVG**IP**A**A** in H7 and **M**GV**SS**LGVMT**N** in H8, as the well characterized Cu^{+}-ATPases of Wilson and Menkes diseases (Bull & Cox, 1994; Bull *et al*., 1993; Petrukhin *et al*., 1994; Vulpe *et al*., 1993).

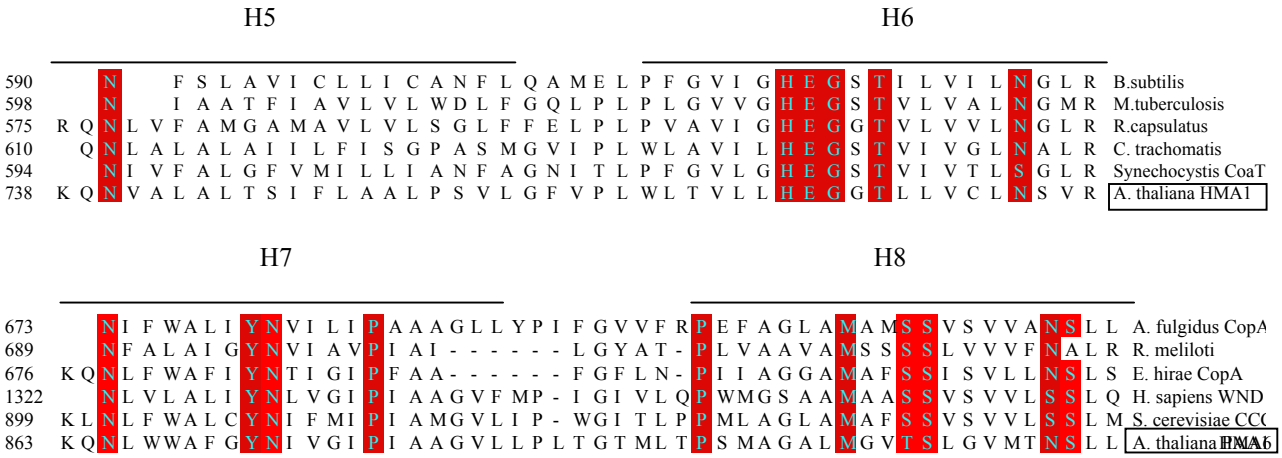

Figure 4: Alignments of H5 and H6 of HMA1 and H7 and H8 of HMA6 with functionally characterized P_{1B}-ATPases. The signature sequences are shown in red boxes. HMA1 presents the consensus sequence in H6 found in CoaT, a putative Co^{2+} transporter, and other related proteins, therefore indicating it as a putative Co^{2+} transporter. HMA6 shares homology in H7 and H8 with members of subgroup 1B-1, WND from humans, CCC2 from yeast and CopA from *A.fulgidus*.

Cloning of HMA1 and HMA6 in pBADTOPO

DNA sequences for HMA1 and HMA6 genes were obtained through GenBank. To clone the open reading frames (ORFs) of HMA1 and HMA6, total RNA from *Arabidopsis thaliana* leaves was extracted, and cDNAs were obtained by reverse transcription using an OligodT primer. The resulting cDNAs were amplified by two rounds of polymerase chain reaction (PCR),

first using primers annealing in 5' and 3' untranslated regions of each of the two transcripts, and the second round with primers annealing at the ends of each ORF.

The resulting ORFs were ligated to the prokaryotic expression vector pBAD-TOPO (Invitrogen) and sequenced. The sequences obtained were aligned with the predicted sequences from GenBank. No mutations were observed and proper in frame translation in bacteria was to be expected for the two proteins (not shown). The resulting constructs were introduced in TOP10 *E.coli* cells, and expression was induced by adding arabinose to exponentially growing cultures.

HMA6 was expressed successfully, although HMA1 could not be detected by immunoblotting. Five other strains were transformed with HMA1-pBADTOPO construct, but HMA1 was not expressed in any of the strains. *E.coli* cells expressing HMA6 were fractionated in soluble and membrane fractions, and it was found that HMA6 was bound to the membrane fraction (Fig 5). Other bands of higher and lower molecular weight were detected by immunoblotting, which could correspond to unspecific binding or degradation products. Membranes of *E.coli* expressing HMA6 were tested for ATPase activity in the presence Cu^{+} or Ag^{+}. No metal-stimulated ATPase activity was detected when assayed for these metals, or when assayed with Cd^{2+}, Zn^{2+}, Co^{2+}, Fe^{2+}, Cu^{2+} or Ni^{2+} (not shown). Metal tolerance assays were then performed to test for *in vivo* activity, but no difference in growth was detected between bacteria expressing HMA6 and untransformed *E.coli* grown in toxic metal concentrations (not shown). *ΔcopA* is an *E.coli* strain with a deletion in the CopA Cu^{+}-ATPase, and its growth is inhibited by high Cu^{2+} concentrations. This strain was kindly provided by Dr. Barry P. Rosen, Wayne State University School of Medicine, and also transformed with HMA6-pBADTOPO vector to test for mutant growth complementation in high Cu^{2+} media. No complementation of growth of the mutant was detected in *ΔcopA* cells expressing HMA6 (not shown).

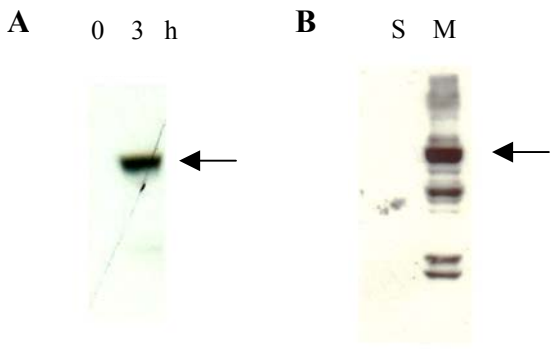

Figure 5: Expression of HMA6 and localization to bacterial membranes. Expression of HMA6 in *E.coli* was induced and protein detected after 3 h in bacterial extracts in blots stained with anti $(His)_6$ antibody (A). Extracts were fractionated in soluble (S) and membrane (M) fractions, and all the protein localized to membrane fraction and detected by the same method (B).

Cloning of HMA1 and HMA6 in pYES2/CT

E.coli, as a heterologous expression system, was not suitable for production of active HMA1 or HMA6, as shown in the previous section. HMA1 and HMA6 are membrane bound eukaryotic proteins, and it is possible the prokaryotic system used would not allow appropriate folding to obtain an active protein. In the case of HMA1, in frame translation was expected by sequence analysis, however no protein was detected.

Given the chosen prokaryotic system did not produce positive results for neither expression of HMA1 nor activity of HMA6, we decided to switch to *Saccaromyces cerevisiae* as

an eukaryotic heterologous system. Consequently, HMA1 and HMA6 genes were cloned in yeast expression vector pYES2/CT under the *GAL1* promoter, and the clones were confirmed by restriction digestion (Fig 6).

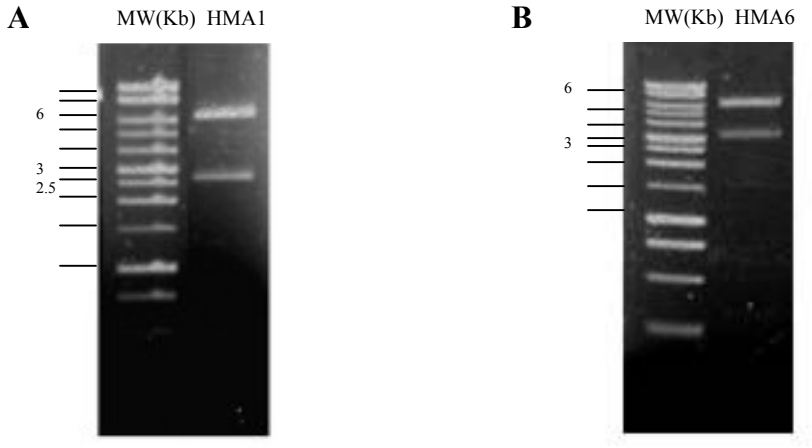

Figure 6: Cloning of HMA1 and HMA6 in pYES2/CT vector. Restriction digestion of resulting plasmids, HMA1-pYES2/CT was cut with SacI and NotI, rendering two fragments of 5963 bp and 2490 bp (A). Restriction digestion of HMA6-pYES2/CT with SacI and NdeI enzymes, produced 5793 bp and 2956 bp fragments (B).

Competent INVSC1 yeast cells were transformed with the resulting vectors by electroporation. Protein expression was induced by diluting an exponentially grown culture in growth media supplemented with galactose. HMA1 was also transformed into *Δcot1* and *Δycf1* strains (BY4743 parental strain), but no protein was detected by immunoblotting in any of the mentioned strains, even after 24 h post induction. The introduction of restriction sites at the 5' end of the cDNA did not affect the open reading frame of the protein, as observed by automated sequencing of the 5' end of the insert (not shown). On the contrary, HMA6 was expressed in yeast at 4 h after induction, and protein was still detected after 24 h. Yeast extracts were

fractionated in soluble and membrane fractions, and all HMA6 protein was bound to membranes (Fig 7).

HMA6 ATPase activity was assayed in yeast membranes in the presence of Cu^{+} and Ag^{+}, but no metal-stimulated activity was found. Other metals like Cu^{2+}, Zn^{2+}, Cd^{2+}, Fe^{2+}, Co^{2+} and Ni^{2+} were assayed, but none of these metals activated HMA6. Given that other ATPases are present in yeast membranes and could account for most of the ATPase activity, it is possible that if HMA6 was active, its activity cannot be detected over the rest due to low expression levels. Therefore, we decided to attempt phosphorylation assays, and detection of protein-bound phosphate in acidic gels, as a more sensitive assay to detect HMA6 activity. Neither Ag^{+} nor Cu^{+} induced phosphorylation was detected in acidic gels (not shown), indicating that HMA6 is not active in yeast membranes.

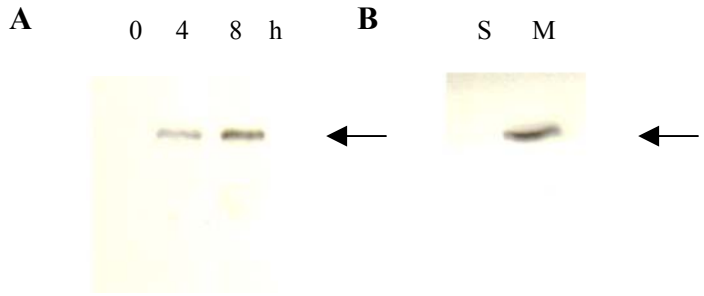

Figure 7: Expression of HMA6 in yeast and localization to membrane fraction. Yeast cells were induced for expression and HMA6 was detected after 4 h in blots stained with anti $(His)_6$ antibody (A). Yeast extracts were fractionated in soluble (S) and membrane (M) fractions, and all protein was detected in membrane fractions by the same method (B).

Considering that the *in vitro* assays, ATPase and phosphorylation, did not render any activity for HMA6, we tried to test if HMA6 could be active *in vivo*. Therefore, two mutant yeast strains in CCC2 Cu^{+}ATPase, *Δccc2* 2809 and *Δccc2* BY4743, were obtained. No

complementation of yeast growth was observed when yeast strain *Δccc2* 2809 was grown in 60 μM BSDS plus 60 μM BCS, or when *Δccc2* BY4743 strain was grown in 30 μM BSDS or 300 μM BCS. The BSDS and BCS concentrations that inhibited mutants over WT were determined experimentally. Another yeast strain defective in FET3 protein, *Δfet3*, is known to accumulate copper when grown in high concentrations of copper. No complementation of growth was observed when yeast cells were grown in up to 4 mM $CuSO_4$ in the media. Both these results indicate that HMA6 is not active in the yeast system.

Since HMA6 is targeted to chloroplast (Shikanai *et al.*, 2003), lack of removal of the transit peptide, incorrect folding or absence of cofactors only present in chloroplasts could account for the lack of activity obtained. An alternative assay could include cloning HMA6 in pYES2/CT without the transit peptide and test for expression and activity.

Transcript levels in plant organs and in seedlings upon metal stress

The expression pattern of these proteins is directly related to their role *in planta*. Moreover, changes in transcript level when plants are grown in metal excess could also indicate if they are involved in metal tolerance mechanisms. Therefore, we determined HMA1 and HMA6 expression pattern in plant organs and in seedlings grown in high metal concentrations by semiquantitative RT-PCR experiments.

To detect expression of HMA1, RNA from different organs of adult plants (6 weeks-old) was reverse transcribed and PCR amplified. HMA1 is expressed in all organs tested except for roots (Fig 8A). This might indicate a role in aerial parts of the plant for metal transport. To determine if HMA1 transcript level is affected by metal stress, seedlings were grown in MS plates plus addition of 0.1 mM $CuSO_4$, 0.25mM $ZnSO_4$, 0.25 mM $CdCl_2$, 0.25mM $NiSO_4$, 0.25 mM $CoCl_2$, 0.5mM $MnCl_2$ and 0.1mM $AgNO_3$. Metal ion concentrations were selected after a

screening for levels that would inhibit root growth without impairing completely seedling development (not shown). Nine days after germination, seedlings were harvested, RNA extracted and transcript level determined by RT-PCR. The addition of the different metal concentrations did not affect the germination rate (not shown). HMA1 expression did not vary significantly in the different metal concentrations tested, although an increase in expression in media with high Cu^{2+} and Co^{2+} and a decrease at high Zn^{2+} and Ni^{2+} concentration was observed (Fig 8B).

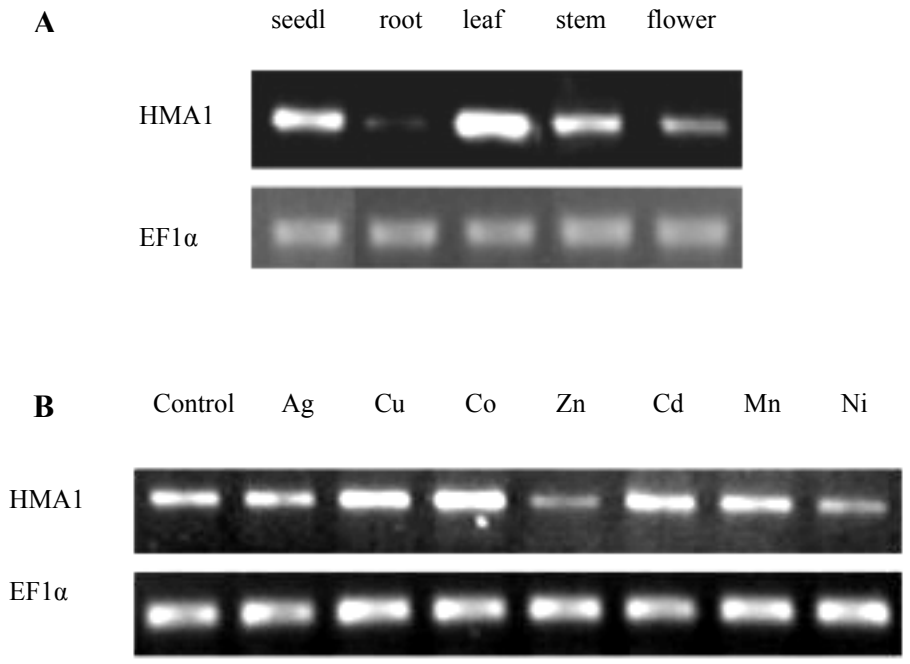

Figure 8: HMA1 transcript levels in different plant organs (A) and in seedlings grown in high metal concentrations (B) In A, RNA was extracted 9 days after germination from (9 DAG) seedlings, and roots, leaves, stems and flowers of 6-week old plants, reversed transcribed and PCR amplified. In B, the same protocol was used for RNA extracted from 9 DAG-old seedlings grown in MS media plus addition of different metals. In both cases, amplification of EF1α transcription factor was used as a control of equal loading and initial amount of DNA in the PCR reaction.

HMA6 transcript level was determined by RT-PCR in different plant organs (Figure 9A). HMA6 is expressed in all organs tested, suggesting ubiquitous function in plants. To test the effect of metal stress on HMA6 expression, transcript levels were determined in seedlings grown at different metal concentrations by semiquantitative RT-PCR. Transcript levels were higher in media with 0.1 mM $CuSO_4$ concentration, suggesting HMA6 might be involved in tolerance to high copper concentrations (Figure 9B).

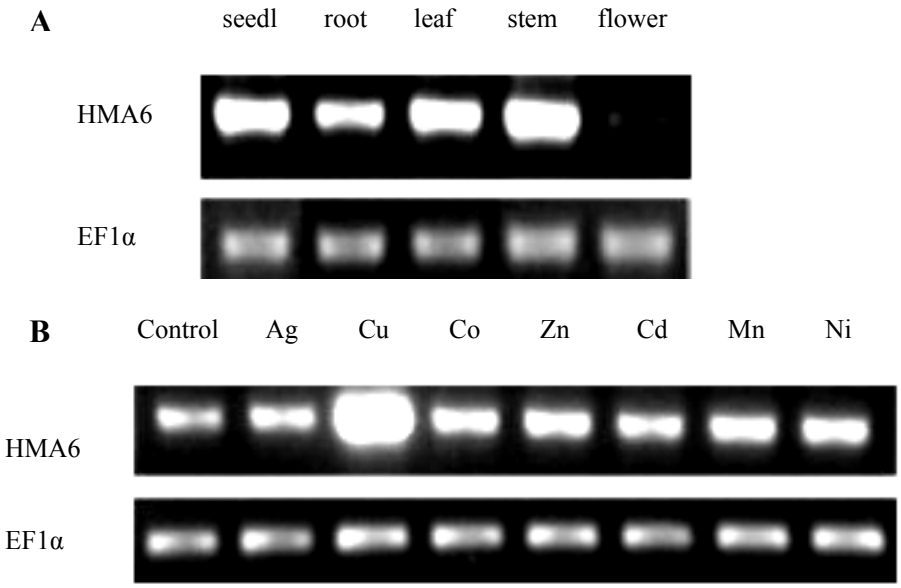

Figure 9: HMA6 transcript levels in different plant organs (A) and in seedlings grown in high metal concentrations (B) In A, RNA was extracted from seedlings, roots, leaves, stems and flowers of 6-week old plants, reversed transcribed and PCR amplified. In B, the same protocol was used but RNA was extracted from 9 DAG-old seedlings grown in MS media addition of different metals. In both cases, amplification of EF1α transcription factor was used as a control.

Screening for homozygous plants for T-DNA insertions

With the goal of understanding the effect of knocking out HMA1 and HMA6 genes in plant growth and development, seed stocks of *Arabidopsis thaliana* lines were analyzed for T-DNA insertions in HMA1 and HMA6 genes.

The Salk Institute is carrying out a high throughput project for the production of T-DNA insertion lines in *Arabidopsis thaliana*. The resulting lines are then screened to detect gene hits for insertions. This information is then added to a database that can be accessed through their website (http://signal.salk.edu/cgi-bin/tdnaexpress). If there are hits in the genes of interest, the seeds can be obtained through the Arabidopsis Biological Resource Center (Ohio State University, Columbus, OH).

A search for T-DNA insertion hits was conducted, and two lines for each HMA1 and HMA6 were ordered. For HMA1, one line presented an insertion in the first exon (stock SALK_088042) and the other in third intron (stock SALK_043265). For HMA6, T-DNA insertion was localized in the third intron (SALK_072581) or in the exon number one (SALK_109629).

Plants from the insertion lines SALK_088042 (HMA1), SALK_043265 (HMA1), SALK_072581 (HMA6) and SALK_109629 (HMA6) were grown in soil for two weeks. A disc was pinched out from one leaf of each plant and genomic DNA was extracted. Plant genomic DNA was used as a template for PCR amplification for T-DNA insertion screening. This screening was done by using two sets of primers; one set consisted of two primers annealing to the gene sequence, flanking the insertion site. This set of primers amplifies only the expected size if there is no T-DNA insertion. In the other set of primers, one of the primers anneals to the gene sequence and the other to the T-DNA. Amplification of the expected size fragment in this

case would indicate the presence of the T-DNA in the expected site. By this screening, three possible outcomes can result: if only a PCR amplification is obtained with the first set of primers, then the plant is wild type; if fragments are obtained with both sets of primers, then the plant is heterozygous; if only amplification with the second set of primers is obtained, then the plant is homozygous for the T-DNA insertion and hence, a knock out in the gene. The knock out is then confirmed by RT-PCR, where no transcript is expected. A scheme of the screening process is shown in Fig 10 for the line SALK_088042. The first set of primers are represented by *a* and *b*, and the second set by *b* and *c*.

A PCR screening was conducted in plants of HMA6 insertion lines SALK_072581 and SALK_109629. Screening of the former only retrieved wild type and heterozygous plants (61% and 39%, respectively, n=41 plants), while the latter, only wild type plants. Other researchers working on the same lines obtained similar results (Torres and Ward, personal communication). It is likely that the in line SALK_109629, the insertion was not in the HMA6 gene, while for SALK_072581, it is apparent the homozygous is lethal. For the latter line, fourteen siliques from four heterozygous plants were screened for 25% dead embryos or 50% less ovules (indicators of embryo lethality and female sterility, respectively). Most of embryos were alive and siliques contained >90% alive ovules (not shown), indicating homozygous plants were neither embryo lethal nor female sterile for this line. This result should be confirmed by similar analysis of other insertion lines.

When HMA1 lines were screened for homozygous, only one plant out of twenty sowed seeds from line SALK_043265 germinated, and those plants were wild type. Another T-DNA insertion line in HMA1 gene, SALK_088042, was screened by PCR and homozygous plants

were found. The absence of HMA1 transcript was further confirmed by RT-PCR (Fig 10) and this line was hence named *hma1-1*.

hma1-1 plants showed similar morphology than wild type plants, thus indicating that HMA1 is not essential for normal plant growth and development. HMA1 transcript was detected as a faint band in homozygous plants when RT-PCR was done at 30 cycles of PCR (Fig 10), and remained with the same intensity up until 35 cycles. However, HMA1 transcript levels in the *hma1-1* line are significantly lower than WT and heterozygous plants, suggesting *hma1-1* might be a knock down instead of a knock out. We continued to characterize this mutant to determine if the knock down in HMA1 gene could have an effect on plant growth, chlorophyll and metal content, and in the expression of other proteins related to metal homeostasis.

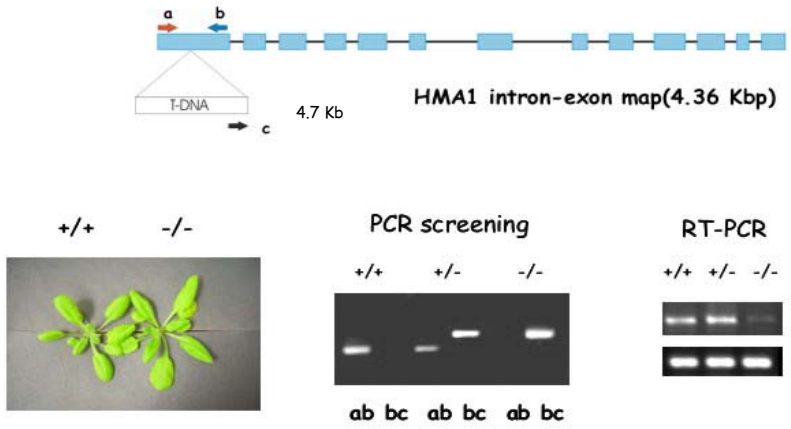

Figure 10: Isolation of *hma1-1* mutant line by PCR and RT-PCR. The intron-exon map of HMA1 is shown at the top of the figure, with the location of the T-DNA insertion in the first exon. Wild type (+/+) and homozygous plants (-/-) show no significant morphological differences (bottom, left panel). In the bottom, center, PCR screening of genomic DNA was done using primer combinations a-b (5HMA1-3HMA104, respectively) or b-c (3LBb1 and 3HMA104, respectively). Primer combination a-b should amplify a band of approximately 252 bp in wild type plants, while b-c should amplify a 450 bp band in the T-DNA insertion mutants. Homozygous plants for insertion in HMA1 exon were confirmed by RT-PCR (bottom, right).

Characterization of hma1-1 *mutant*

Macroscopically, *hma1-1* plants grow in a similar fashion than wild type plants (Fig 10). However, *hma1-1* shows lower weight and less total chlorophyll content than WT plants (Fig 11).

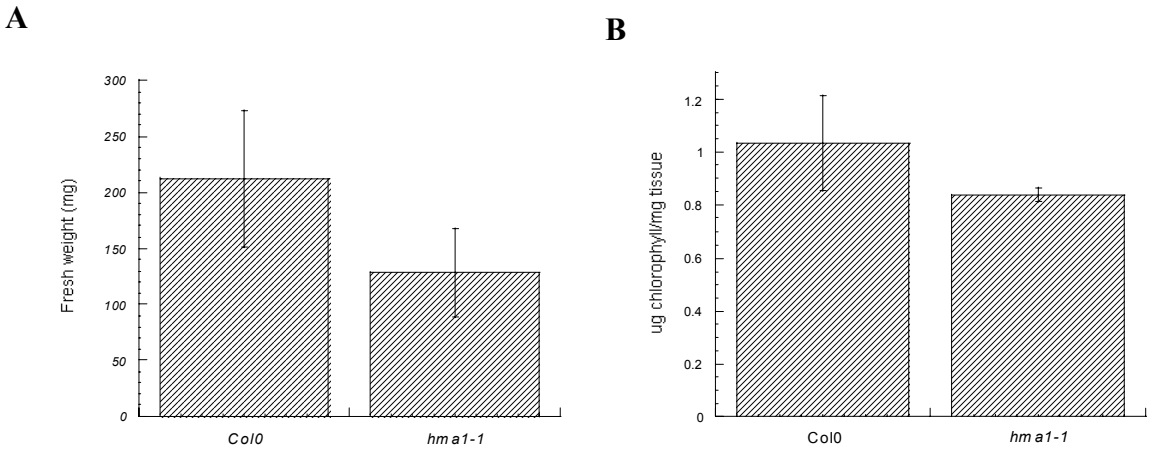

Figure 11: Measurement of fresh weight (A) and total chlorophyll content (B) in Col 0 and *hma1-1* plants. (A) Mean ± SD, n=20. (B) Total chlorophyll content was determined as described by Wu *et al* (2002). Mean ± SD, n=3.

To determine if mutant plants could have impaired growth under metal stress or deficiency, WT and *hma1-1* seedlings were grown in plates with MS media in metal deficiency, or supplemented with excess of either $CuSO_4$, $ZnSO_4$, $CdCl_2$, $NiSO_4$, $CoCl_2$, $MnCl_2$ and $AgNO_3$. The metal concentrations used were determined based on concentration that would inhibit seedling root growth significantly in wild type plants. Eight days after germination, root length of seedlings was measured (Fig 12).

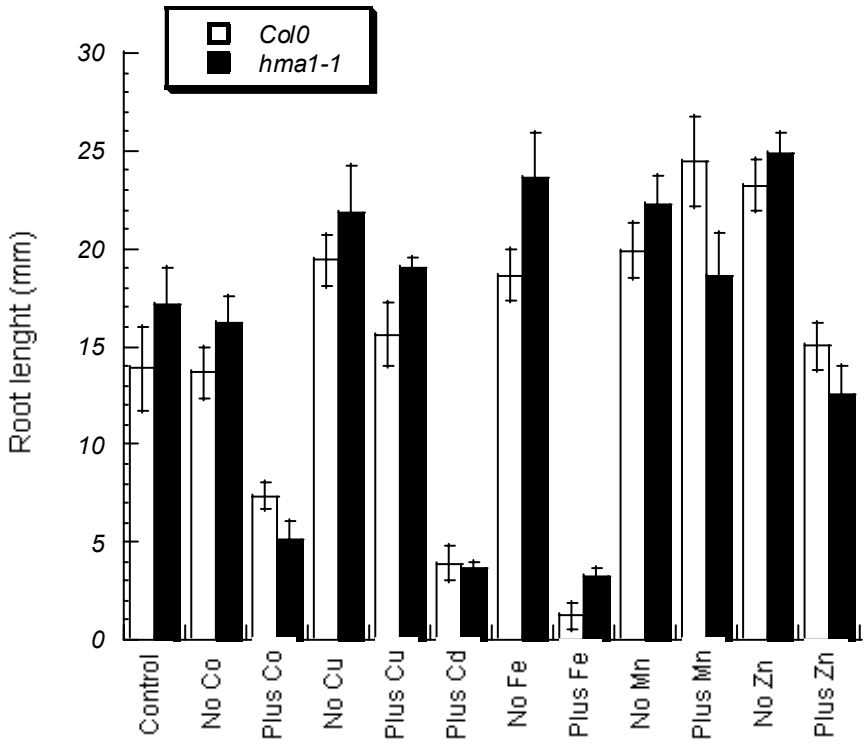

Figure 12: Root length of seedlings grown in metal deficiency or with excess metal in the growth media. Mean ± SD, n=20.

As shown in Fig 12, mutant seedlings grown in control media show longer roots than WT, and this pattern is observed in all conditions tested except for high Cd^{2+} concentration, where root lengths are not significantly different, and in high Co^{2+}, Mn^{2+} and Zn^{2+}, where roots are shorter in mutants than in WT plants ($P<0.05$). This result suggests that absence of HMA1 has an effect on metal homeostasis mechanisms, and HMA1 could be involved in metal tolerance or regulation of metal levels.

To determine if metal levels are affected in mutant plants, whole plants (rosette stage), leaves and roots form WT and *hma1-1* plants were analyzed for iron, zinc and manganese content by atomic absorption spectroscopy. These determinations were done per dry weight of

tissue given the differences in fresh weight obtained for WT and *hma1-1* plants. Mutant plants have higher zinc, manganese and iron contents than WT and mutant plants (Fig 13). This indicates that mechanisms for maintenance of homeostatic iron, zinc and manganese levels are affected in *hma1-1* plants, and that HMA1 could play an essential role in maintaining physiological levels of a range of different metals in *A. thaliana*.

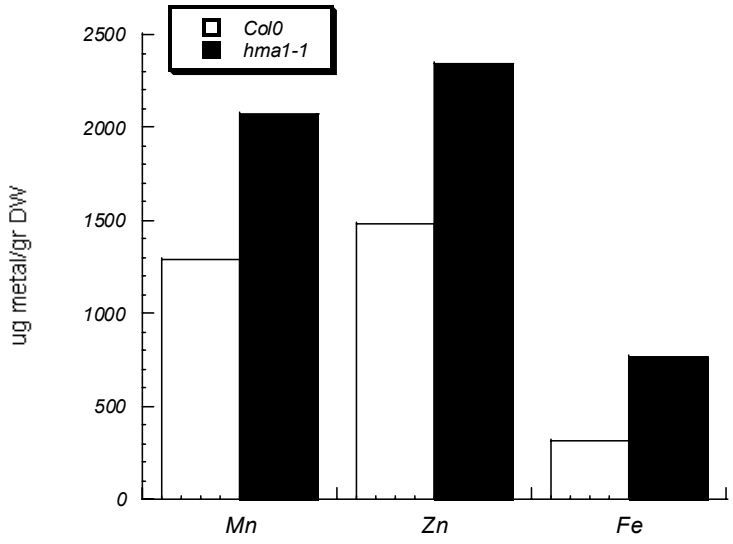

<u>Figure 13:</u> Manganese, zinc and iron content in whole plants (rosette stage) of WT (Col0) and *hma1-1* plants per dry weight.

Metal concentrations were also determined in leaves and roots of rosette stage plants. These determinations were done per fresh weight, and then normalized to obtain metal content per plant (Fig 14). Zinc and manganese accumulation appears to be located mainly in leaves, while the levels in roots remained the same in WT and mutant plants. This also correlates with the expression of HMA1 in aerial parts of the plant, being only leaves in rosette stage plants. The results obtained with iron levels were somewhat striking. Mutant plants accumulate more iron

than WT plants. However, when iron levels are measured in leaves and roots, mutant leaves have less iron than WT, although mutant roots have comparable iron levels than WT plants. Therefore, it is not clear how iron homeostasis mechanisms are affected in *hma1-1* plants.

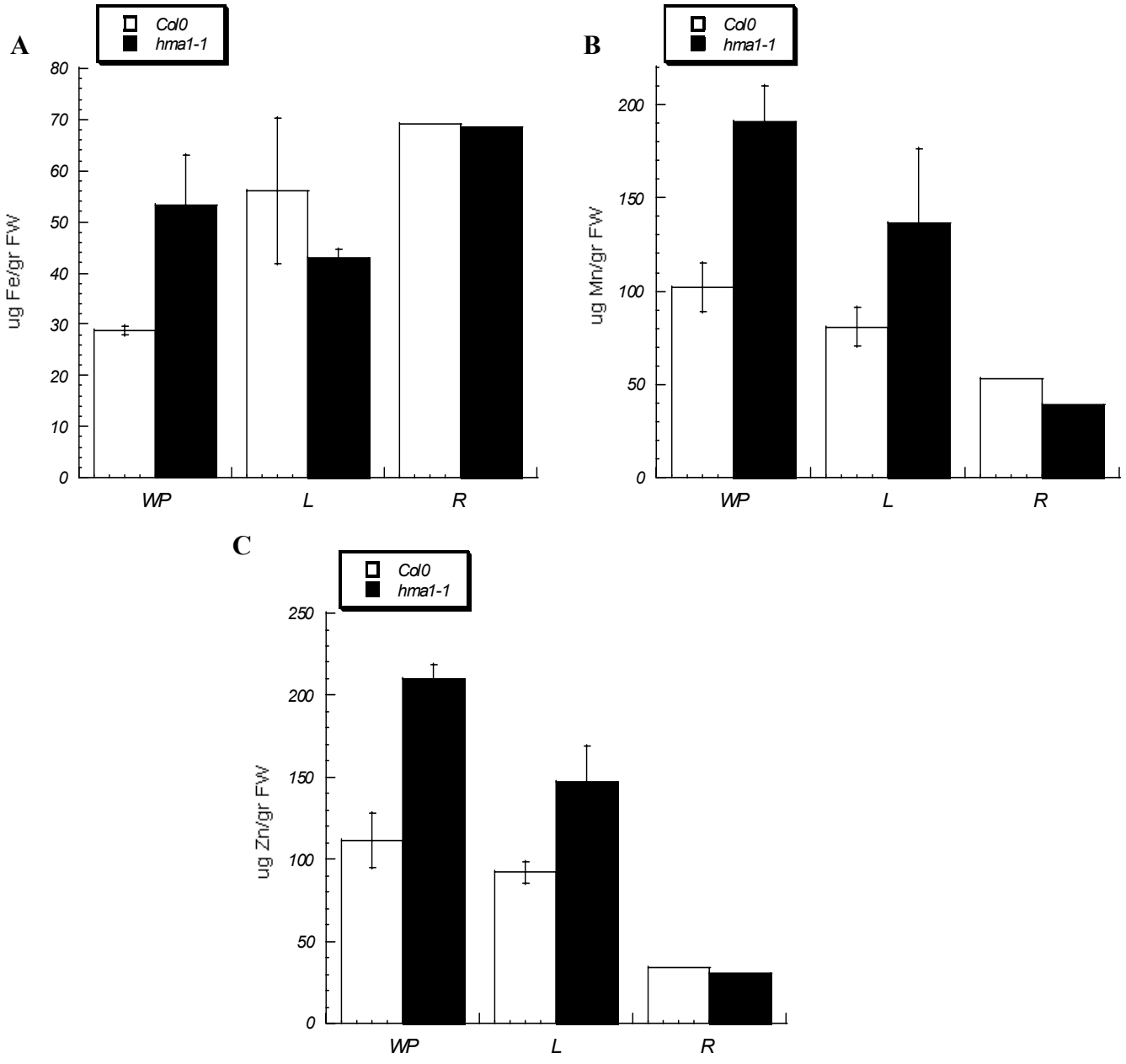

Figure 14: Iron (A), Manganese (B) and Zinc (C) levels per plant. Total metal amount was normalized to represent metal content per plant. *WP*: whole plant; *L*: leaves; *R*: roots. Mean ± SD, n=2.

To test the effect of knocking down HMA1 gene on the expression of some *Arabidopsis* proteins related to metal homeostasis, expression of the metallothioneins MT1a, MT1c, MT2a and MT2b; the phytochellatin synthases PCS1 and PCS2, and other related HMAs, HMA3 and HMA4, was determined by semiquantitative RT-PCR (Fig 15).

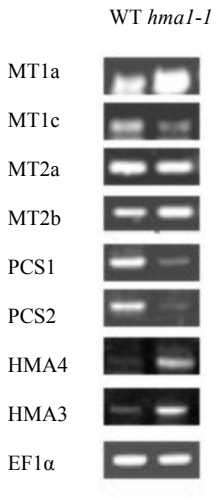

Figure 15: Transcript levels of proteins related to heavy metal homeostasis in WT and *hma1-1* plants. Expression of metallothioneins 1a, 1c, 2a and 2b, Phytochellatin synthases 1 and 2, and Heavy Metal ATPases 3 and 4 from *Arabidopsis*, was measured by RT-PCR.

In *hma1-1* plants, MT1a and MT2b are upregulated, MT1c levels are lower in mutant plants while MT2a expression appears not to change compared to expression in WT plants. PCS1 and PCS2, both are downregulated in the mutant plants. HMA3 and HMA4, two proteins that apparently transport Zn^{2+}/Cd^{2+}/Pb^{2+}, are upregulated in mutant plants.

It is apparent that knocking down HMA1 gene has a significant effect on many metal homeostasis components. Mutant plants contain less chlorophyll, are smaller and have increased levels of metals compared to WT plants. Also, proteins that have been directly involved with metal tolerance and scavenging in cells have altered expression patterns. However, to interpret

these results in the context of the role of HMA1 in all of these processes, functional studies with isolated protein need to be performed.

DISCUSSION

The knowledge of plant metal homeostasis is crucial to understand how plants can grow in highly polluted soils, or how to enrich mineral content of foodstuffs. In this work we show the expression of HMA1 and 6 in different plant organs and upon metal stress by RT-PCR analysis, and the effect of HMA1 mutation on plant metabolism. The results obtained in this work indicate that HMA1 and HMA6 are essential components of metal homeostasis in *Arabidopsis thaliana*, although the mechanism by which metal concentrations are regulated is still to be determined by complementing the results obtained in this work with functional data.

Cloning of HMA1 and HMA6 genes

HMA1 was expressed in neither bacteria nor yeast. Analysis of the sequence of the cDNA indicates this protein has the correct frame for translation when present in pBADTOPO or in pYES2/CT. It could be possible that during or after transcription and/or translation, the transcript or the protein are targeted for degradation.

HMA6 was successfully expressed in bacteria and in yeast, and located to membranes in both systems, although protein was non functional. Several assays including ATPase, metal tolerance, phosphorylation and mutant complementation were performed but no metal stimulated activity was detected. It could be possible that given HMA6 is a chloroplast bound protein, presence of chloroplastic cofactors are necessary for its activation. Additionally, lack of removal of the transit peptide could interfere with proper folding and activity. Future experiments could aim to clone HMA6 without the transit peptide and determine if the protein is then functional.

Expression of HMA1 and HMA6 in organs and upon metal stress

HMA1 was expressed in all organs except for roots. This indicates a role in metal transport in aerial parts, probably xylem unloading and phloem and leaf cells loading. HMA1 transcript appears not to vary significantly upon stress provoked by different metals in seedlings, although a decrease in HMA1 expression upon Zn^{2+} and Ni^{2+} stress and an increase upon Cu^{2+} and Co^{2+} stress was observed by RT-PCR.

HMA6 is proposed to transport Cu^{+}/Ag^{+}. Its transcript was found in all organs tested. Its presence in roots in levels comparable to those in leaves is striking since this protein is apparently located in chloroplasts (Shikanai *et al.*, 2003). It could be possible that this protein is targeted to another cellular compartment in roots, however the mechanisms of targeting should be elucidated given the presence of a chloroplast signal target peptide in HMA6 structure. The presence of its transcript in every organ tested indicates that this protein might be a ubiquitous component of metal homeostasis in the whole plant body. When seedlings were grown in 0.1 mM $CuSO_4$, HMA6 was also overexpressed. This result contradicts the one obtained by Tabata *et al* (1997), where they did not observe changes in transcript level in $CuSO_4$ media at 0.01 and 1 mM $CuSO_4$. In their report, plants were treated with $CuSO_4$ in media for 24 h and RNA from whole plants was extracted. Here, plants were germinated and grown for 12 days in media containing metal. It is possible the longer metal treatment could account for the increased levels of transcript found in this work

Together, these results indicate HMA1 and HMA6 to be ubiquitous components of plant metal homeostasis, and HMA1 to be involved in tolerance to a range of metals when present in high concentrations. HMA6 appears to be involved in tolerance to high Cu^{2+} concentrations, instead.

Characterization of* hma1-1 *insertion mutant

To understand how essential these proteins are for plant metabolism, analysis of insertion mutants for the genes of interest was initiated. Two insertion lines for HMA1 gene and two for HMA6 gene were obtained and screened for homozygous in the genes of interest.

When HMA6 insertion lines were screened for homozygous, with one of the lines (SALK_109629) all wild type genotypes were obtained, while for the other line (SALK_072581), wild type and heterozygous genotypes were obtained, though no homozygous. Other investigators working with the same lines had similar results (Torres and Ward, personal communication). Non-obtaining homozygous could be explained if the homozygous is embryo lethal or the female is sterile. Siliques were dissected and embryos counted to determine if 25% of embryos were dead or if female were sterile. All embryos were alive and ovules were viable, therefore it is apparent that lethality is neither due to embryo lethality nor female sterility. However, analysis of other insertion lines should be done to confirm these results.

For HMA1 gene, homozygous for one insertion line was obtained, *hma1-1* (SALK_088042, this study), while for the other line (SALK_043265), only 5% of plants actually germinated when planted for initial screening, and those plants were wild type. It has been observed that the insertion information at the Salk Institute database has a 70% error rate (Ward, personal communication). Therefore, it is possible this line was not a mutant, or it might have had more than one insertion, thus affecting plant germination.

Mutant *hma1-1* plants show similar morphology, although smaller size and chlorophyll content than WT plants. *hma1-1* plants also contained higher Zn^{2+}, Mn^{2+} and Fe^{2+} content than WT plants, and Zn^{2+} and Mn^{2+} accumulation was mainly in leaves, while metal levels in roots remained unchanged. The results obtained with Fe^{2+} were somewhat striking, given that the

content in whole plants was higher than in WT plants, although in leaves smaller than WT and unchanged in roots. The mechanisms of iron regulation by HMA1 are still to be determined. This results suggest that HMA1 act in maintaining metal concentrations in leaves, at least for the metals tested.

Altered expression of proteins related to metal homeostasis was found in *hma1-1* plants compared to WT plants. Metallothioneins 1a and 2b were overexpressed, while 1c was underexpressed and 2a remained unchanged. Phytochellatin synthases 1 and 2 had lower transcript levels than WT plants, and HMA3 and HMA4, two P_{1B}-ATPases belonging to subgroup 1B-2, are overexpressed in *hma1-1* plants. This results show that HMA1 has a pivotal role in maintaining metal concentrations within homeostatic ranges; knock down of this gene generated multiple responses in the expression of proteins involved in metal homeostasis.

These results altogether indicate that HMA1 is an essential component of metal homeostasis in *Arabidopsis thaliana*, and its role might be direct or through other metal regulating proteins. In spite the specificity of HMA1 has not yet been determined, results obtained in this work indicate HMA1 as a necessary component for maintenance of concentrations of a broad range of metals, and that its function is mainly exerted in leaves. Functional studies with isolated protein are necessary to elucidate the mechanisms by which this regulation of metal concentrations is being produced.

BIBLIOGRAPHY

Alonso, J.M., Anna N. Stepanova, Thomas J. Leisse, Christopher J. Kim, Huaming Chen, Paul Shinn, Denise K. Stevenson, Justin Zimmerman, Pascual Barajas, Rosa Cheuk, Carmelita Gadrinab, Collen Heller, Albert Jeske, Eric Koesema, Cristina C. Meyers, Holly Parker, Lance Prednis, Yasser Ansari, Nathan Choy, Hashim Deen, Michael Geralt, Nisha Hazari, Emily Hom, Meagan Karnes, Celene Mulholland, Ral Ndubaku, Ian Schmidt, Plinio Guzman, Laura Aguilar-Henonin, Markus Schmid, Detlef Weigel, David E. Carter, Trudy Marchand, Eddy Risseeuw, Debra Brogden, Albana Zeko, William L. Crosby, Charles C. Berry, and Joseph R. Ecker. 2003. Genome-Wide Insertional Mutagenesis of *Arabidopsis thaliana*. *Science* **301:**653-657

Argüello, J.M. 2003. Identification of ion selectivity determinants in heavy metal transport P_{1B}-ATPases. *J Membr Biol* **195:** 93-108

Axelsen, K.B., Palmgren, M.G. 1998. Evolution of substrate specificities in the P-type ATPase superfamily. *J Mol Evol* **46:**84-101.

Axelsen, K.B., Palmgren, M.G. 2001. Inventory of the superfamily of P-type ion pumps in *Arabidopsis*. *Plant Physiol* **126:**696-706.

Baxter I, T.J., Sussman MR, Boutry M, Palmgren MG, Gribskov M, Harper JF, Axelsen KB. 2003. Genomic comparison of P type ATPase Ion Pumps in *Arabidopsis* and rice. *Plant Physiol* **132:**618-628

Bissig, K.D., Wunderli-Ye, H., Duda, P.W., Solioz, M. 2001. Structure-function analysis of purified *Enterococcus hirae* CopB copper ATPase: effect of Menkes/Wilson disease mutation homologues. *Biochem J* **357:**217-23.

Bloss, T., Clemens, S., Nies, D.H. 2002. Characterization of the ZAT1p zinc transporter from *Arabidopsis thaliana* in microbial model organisms and reconstituted proteoliposomes. *Planta* **214:**783-91.

Bradford, M.M. 1976. A rapid and sensitive method for the quantitation of microgram quantities of protein utilizing the principle of protein-dye binding. *Anal Biochem* **72:**248-254

Bull, P.C., Cox, D.W. 1994. Wilson disease and Menkes disease: new handles on heavy-metal transport. *Trends Genet* **10:**246-52.

Bull, P.C., Thomas, G.R., Rommens, J.M., Forbes, J.R., Cox, D.W. 1993. The Wilson disease gene is a putative copper transporting P-type ATPase similar to the Menkes gene [published erratum appears in Nat Genet 1994 Feb;6(2):214]. *Nat Genet* **5:**327-337

Clemens, S. 2001. Molecular mechanisms of plant metal tolerance and homeostasis. *Planta* **212:**475-86.

Cobbett, C.S. 2000. Phytochelatin biosynthesis and function in heavy-metal detoxification. *Curr Op Plant Biol* **3:**211-216

Cobbett, C.S., Hussain, D., Haydon, M.J. 2003. Structural and functional relationships between type 1B heavy metal-transporting P-type ATPases in *Arabidopsis*. *New Phytologist* **159:**315-321

Cohen, C.K., Fox, T.C., Garvin, D.F., Kochian, L.V. 1998. The role of iron-deficiency stress responses in stimulating heavy-metal transport in plants. *Plant Physiol* **116:**1063-72.

Curie, C., Alonso, J.M., Le Jean, M., Ecker, J.R., Briat, J.F. 2000. Involvement of NRAMP1 from *Arabidopsis thaliana* in iron transport. *Biochem J* **347 Pt 3:**749-55.

Edwards, K., Johnstone, C., Thompson, C. 1991. A simple and rapid method for the preparation of plant genomic DNA for PCR analysis. *Nucleic Acids Res* **19:**1349

Eide, D., Broderius, M., Fett, J., Guerinot, M.L. 1996. A novel iron-regulated metal transporter from plants identified by functional expression in yeast. *Proc Natl Acad Sci U S A* **93:**5624-8.

Fan B, R.B. 2002. Biochemical characterization of CopA, the *Escherichia coli* Cu(I)-translocating P-type ATPase. *J Biol Chem* **277:**46987-46992

Garcia-Hernandez, M., Murphy, A., Taiz, L. 1998. Metallothioneins 1 and 2 have distinct but overlapping expression patterns in *Arabidopsis*. *Plant Physiol* **118:**387-97.

Gravot, A., Lieutaud, A., Verret, F., Auroy, P., Vavasseur A., Richaud, P. 2004. AtHMA3, a plant P_{1B}-ATPase, functions as a Cd/Pb transporter in yeast. *Febs Lett* **561:**22-28

Grotz, N., Fox, T., Connolly, E., Park, W., Guerinot, M.L., Eide, D. 1998. Identification of a family of zinc transporter genes from *Arabidopsis* that respond to zinc deficiency. *Proc Natl Acad Sci U S A* **95:**7220-4.

Hall, J.L. 2002. Cellular mechanisms for heavy metal detoxification and tolerance. *J Exp Bot* **53:**1-11.

Hamer, D.H. 1986. Metallothionein. *Annu Rev Biochem* **55:**913-51

Hamza, I., Schaefer, M., Klomp, L.W., Gitlin, J.D. 1999. Interaction of the copper chaperone HAH1 with the Wilson disease protein is essential for copper homeostasis. *Proc Natl Acad Sci U S A* **96:**13363-8.

Himelblau, E., Mira, H., Lin, S.J., Culotta, V.C., Penarrubia, L., Amasino, R.M. 1998. Identification of a functional homolog of the yeast copper homeostasis gene ATX1 from *Arabidopsis. Plant Physiol* **117:**1227-34.

Hirayama, T., Kieber, J.J., Hirayama, N., Kogan, M., Guzman, P., Nourizadeh, S., Alonso, J.M., Dailey, W.P., Dancis, A., Ecker, J.R. 1999. RESPONSIVE-TO-ANTAGONIST1, a

Menkes/Wilson disease-related copper transporter, is required for ethylene signaling in *Arabidopsis. Cell* **97:**383-93.

Kampfenkel, K., Kushnir, S., Babiychuk, E., Inze, D., Van Montagu, M. 1995. Molecular characterization of a putative *Arabidopsis thaliana* copper transporter and its yeast homologue. *J Biol Chem* **270:**28479-86.

Korshunova, Y.O., Eide, D., Clark, W.G., Guerinot, M.L., Pakrasi, H.B. 1999. The IRT1 protein from *Arabidopsis thaliana* is a metal transporter with a broad substrate range. *Plant Mol Biol* **40:**37-44.

Laemmli, U.K. 1970. Cleavage of structural proteins during the assembly of the head of bacteriophage T4. *Nature* **227:**680-5.

Li, L., He, Z., Pandey, G.K., Tsuchiya, T., Luan, S. 2002. Functional cloning and characterization of a plant efflux carrier for multidrug and heavy metal detoxification. *J Biol Chem* **277:**5360-8.

Lin, S.J., Pufahl, R.A., Dancis, A., TV, O.H., Culotta, V.C. 1997. A role for the *Saccharomyces cerevisiae* ATX1 gene in copper trafficking and iron transport. *J Biol Chem* **272:**9215-20

Lutsenko, S., Kaplan, J.H. 1995. Organization of P-type ATPases: Significance of structural diversity. *Biochem* **34:**15607-15613

Lutsenko, S., Petrukhin, K., Cooper, M.J., Gilliam, C.T., Kaplan, J.H. 1997. N-terminal domains of human copper-transporting adenosine triphosphatases (the Wilson's and Menkes disease proteins) bind copper selectively *in vivo* and *in vitro* with stoichiometry of one copper per metal-binding repeat. *J Biol Chem* **272:**18939-18944

Lutsenko, S., Petris, MJ. 2002. Function and regulation of the mammalian copper- transporting ATPases: Insights from biochemical and cell biological approaches. *J Membr Biol* **191:**1-12

Mana-Capelli, S., Mandal, A.K., Arguello, J.M. 2003. *Archaeoglobus fulgidus* CopB Is a Thermophilic Cu^{2+}-ATPase: functional role of its histidine-rich N-terminal metal binding domain. *J Biol Chem* **278:**40534-40541

Mandal, A.K., Cheung, W.D., Arguello, J.M. 2002. Characterization of a Thermophilic P-type Ag^{+}/Cu^{+}-ATPase from the Extremophile *Archaeoglobus fulgidus*. *J Biol Chem* **277:**7201-7208

Mandal AK., Arguello J.M. 2003. Functional roles of metal binding domains of the *Archaeoglobus fulgidus* Cu(+)-ATPase CopA. *Biochemistry* **42:**11040-7

Marschner, H. 1995. Mineral nutrition of higher plants. Academic Press, London ; San Diego

Maser, P., Thomine, S., Schroeder, J.I., Ward, J.M., Hirschi, K., Sze, H., Talke, I.N., Amtmann, A., Maathuis, F.J., Sanders, D., Harper, J.F., Tchieu, J., Gribskov, M., Persans, M.W., Salt, D.E., Kim, S.A., Guerinot, M.L. 2001. Phylogenetic relationships within cation transporter families of *Arabidopsis*. *Plant Physiol* **126:**1646-67.

Melchers, K., Weitzenegger, T., Buhmann, A., Steinhilber, W., Sachs, G., Schofer, K.P. 1996. Cloning and membrane topology of a P type ATPase from *Helicobacter pylori*. *J Biol Chem* **271:**446-457

Mills, R.F., Krijger, G.C., Baccarini, P.J., Hall, J.L., Williams, L.E. 2003. Functional expression of AtHMA4, a P_{1B}-type ATPase of the Zn/Co/Cd/Pb subclass. *Plant J* **35:**164-176

Mitra, B., Sharma, R. 2001. The cysteine-rich amino-terminal domain of ZntA, a Pb(II)/Zn(II)/Cd(II)-translocating ATPase from *Escherichia coli*, is not essential for its function. *Biochemistry* **40:**7694-7699

Murphy, A., Taiz, L. 1995. A New Vertical Mesh Transfer Technique for Metal-Tolerance Studies in *Arabidopsis* (Ecotypic Variation and Copper-Sensitive Mutants). *Plant Physiol* **108:**29-38.

Odermatt, A., Suter, H., Krapf, R., Solioz, M. 1993. Primary structure of two P-type ATPases involved in copper homeostasis in *Enterococcus hirae*. *J Biol Chem* **268:**12775-12779

Ortiz, D.F., Ruscitti, T., McCue, K.F., Ow, D.W. 1995. Transport of metal-binding peptides by HMT1, a fission yeast ABC-type vacuolar membrane protein. *J Biol Chem* **270:**4721-8.

Outten, C.E., O'Halloran, T.V. 2001. Femtomolar sensitivity of metalloregulatory proteins controlling zinc homeostasis. *Science* **292:**2488-92.

Paulsen, I.T., Saier, M.H., Jr. 1997. A novel family of ubiquitous heavy metal ion transport proteins. *J Membr Biol* **156:**99-103

Pence, N.S., Larsen, P.B., Ebbs, S.D., Letham, D.L., Lasat, M.M., Garvin, D.F., Eide, D., Kochian, L.V. 2000. The molecular physiology of heavy metal transport in the Zn/Cd hyperaccumulator *Thlaspi caerulescens*. *Proc Natl Acad Sci U S A* **97:**4956-4960

Petrukhin, K., Lutsenko, S., Chernov, I., Ross, B.M., Kaplan, J.H., Gilliam, T.C. 1994. Characterization of the Wilson disease gene encoding a P-type copper transporting ATPase: genomic organization, alternative splicing, and structure/function predictions. *Hum Mol Genet* **3:**1647-56

Pufahl, R.A., Singer, C.P., Peariso, K.L., Lin, S.J., Schmidt, P.J., Fahrni, C.J., Culotta, V.C., PennerHahn, J.E., Ohalloran, T.V. 1997. Metal ion chaperone function of the soluble Cu(I) receptor Atx1. *Science* **278:**853-856

Rae, T.D., Schmidt, P.J., Pufahl, R.A., Culotta, V.C., O'Halloran, T.V. 1999. Undetectable intracellular free copper: The requirement of a copper chaperone for superoxide dismutase. *Science* **284:**805-808

Rauser, W.E. 1999. Structure and function of metal chelators produced by plants: the case for organic acids, amino acids, phytin, and metallothioneins. *Cell Biochem Biophys* **31:**19-48

Rensing, C., Mitra, B., Rosen, B.P. 1997. The zntA gene of *Escherichia coli* encodes a Zn(II)-translocating P-type ATPase. *Proc Natl Acad Sci U S A* **94:**14326-31

Robinson, N.J., Wilson, J.R., Turner, J.S. 1996. Expression of the type 2 metallothionein-like gene MT2 from Arabidopsis thaliana in Zn(2+)-metallothionein-deficient *Synechococcus* PCC 7942: putative role for MT2 in Zn^{2+} metabolism. *Plant Mol Biol* **30:**1169-79.

Rogers, E.E., Guerinot, M.L. 2002. FRD3, a Member of the Multidrug and Toxin Efflux Family, Controls Iron Deficiency Responses in *Arabidopsis*. *Plant Cell* **14:**1787-99.

Rutherford, J.C., Cavet, J.S., Robinson, N.J. 1999. Cobalt-dependent transcriptional switching by a dual-effector MerR-like protein regulates a cobalt-exporting variant CPx-type ATPase. *J Biol Chem* **274:**25827-25832

Sambrook, J., Fritsch, E.F., Maniatis, T. 1989. Molecular cloning. A laboratory Manual. Cold Spring Harbor Laboratory Press, New York

Sarkadi, B.E., A; Foldes-Papp, Z; Gardos, G. 1986. Molecular characterization of the *in situ* red cell membrane calcium pump by limited proteolysis. *J Biol Chem* **261:**9552-9557

Sharma, R., Rensing, C., Rosen, B.P., Mitra, B. 2000. The ATP hydrolytic activity of purified ZntA, a Pb(II)/Cd(II)/Zn(II)-translocating ATPase from *Escherichia coli*. *J Biol Chem* **275:**3873-3878

Shikanai, M.-M., Munekage, Niyogi, Pilon. 2003. PAA1, a P-type ATPase from *Arabidopsis,* Functions in Copper Transport in Chloroplasts. *Plant Cell* **15:**1333-1346

Tabata, K., Kashiwagi, S., Mori, H., Ueguchi, C., Mizuno, T. 1997. Cloning of a cDNA encoding a putative metal-transporting P-type ATPase from *Arabidopsis thaliana*. *Biochim Biophys Acta* **1326:**1-6.

Thomine, S., Wang, R., Ward, J.M., Crawford, N.M., Schroeder, J.I. 2000. Cadmium and iron transport by members of a plant metal transporter family in Arabidopsis with homology to Nramp genes. *Proc Natl Acad Sci U S A* **97:**4991-6.

Tsai, K.J., Lin, Y.F., Wong, M.D., Yang, H.H., Fu, H.L., Rosen, B.P. 2002. Membrane topology of the p1258 CadA Cd(II)/Pb(II)/Zn(II)-translocating P-type ATPase. *J Bioenerg Biomembr* **34:**147-56.

van der Zaal, B.J., Neuteboom, L.W., Pinas, J.E., Chardonnens, A.N., Schat, H., Verkleij, J.A., Hooykaas, P.J. 1999. Overexpression of a novel *Arabidopsis* gene related to putative zinc- transporter genes from animals can lead to enhanced zinc resistance and accumulation. *Plant Physiol* **119:**1047-55.

Vert, G., Briat, J.F., Curie, C. 2001. Arabidopsis IRT2 gene encodes a root-periphery iron transporter. *Plant J* **26:**181-9.

Voskoboinik, I., Mar, J., Strausak, D., Camakaris, J. 2001. The regulation of catalytic activity of the menkes copper-translocating P-type ATPase. Role of high affinity copper-binding sites. *J Biol Chem* **276:**28620-7.

Voskoboinik, I., Strausak, D., Greenough, M., Brooks, H., Petris, M., Smith, S., Mercer, J.F., Camakaris, J. 1999. Functional analysis of the N-terminal CXXC metal-binding motifs in the human Menkes copper-transporting P-type ATPase expressed in cultured mammalian cells. *J Biol Chem* **274:**22008-22012

Vulpe, C., Levinson, B., Whitney, S., Packman, S., Gitschier, J. 1993. Isolation of a candidate gene for Menkes disease and evidence that it encodes a copper-transporting ATPase. *Nat Genet* **3:**7-13

Williams, L.E., Pittman, J.K., Hall, J.L. 2000. Emerging mechanisms for heavy metal transport in plants. *Biochim Biophys Acta* **1465:**104-26.

Woeste, K.E., Kieber, J.J. 2000. A strong loss-of-function mutation in RAN1 results in constitutive activation of the ethylene response pathway as well as a rosette-lethal phenotype. *Plant Cell* **12:**443-55.

Wu Z, L.F., Hong B, Young JC, Sussman MR, Harper JF, Sze H. 2002. An endoplasmic reticulum-bound Ca(2+)/Mn(2+) pump, ECA1, supports plant growth and confers tolerance to Mn(2+) stress. *Plant Physiol* **130:**128-137

Yoshimizu, T., Omote, H., Wakabayashi, T., Sambongi, Y., Futai, M. 1998. Essential Cys-Pro-Cys motif of *Caenorhabditis elegans* copper transport ATPase. *Biosci Biotechnol Biochem* **62:**1258-1260